TRIBHUVAN UNIVERSITY

INSTITUTE OF ENGINEERING

PULCHOWK CAMPUS

THESIS NO: M-77-MSMDE-2021-2023

Design, Fabrication and Performance Evaluation of Low Speed Open Jet Wind Tunnel for Free Flight Test of a Glider

by

Rakesh Chaudhary

A THESIS SUBMITTED TO THE DEPARTMENT OF MECHANICAL AND AEROSPACE ENGINEERING IN PARTIAL FULFILLMENT OF THE REQUIREMENTS FOR THE DEGREE OF MASTERS OF SCIENCE IN MECHANICAL SYSTEMS DESIGN AND ENGINEERING

DEPATRMENT OF MECHANICAL AND AEROSPACE ENGINEERING

LALITPUR, NEPAL

NOVEMBER, 2023

TRIBHUVAN UNIVERSITY

INSTITUTE OF ENGINEERING

PULCHOWK CAMPUS

DEPARTMENT OF MECHANICAL AND AEROSPACE ENGINEERING

The undersigned certify that they have read, and recommended to the Institute of Engineering for acceptance, a thesis entitled **"Design, Fabrication and Performance Evaluation of Low Speed Open Jet Wind Tunnel for Free Flight Test of a Glider"** submitted by **Rakesh Chaudhary** in partial fulfillment of the requirements for the degree of Master of Science in Mechanical Systems Design and Engineering.

Supervisor, Laxman Poudel. Ph.D.
Professor
Department of Mechanical and Aerospace Engineering

Supervisor, Sudip Bhattrai, Ph.D.
Assistant Professor
Department of Mechanical and Aerospace Engineering

External Examiner, Ashish Manandhar
Maintenance Planning & Control Engineer
Himalaya Airlines

Committee Chairperson, Sudip Bhattrai, Ph.D.
Head of Department
Department of Mechanical and Aerospace Engineering

Tribhuvan University
Institute of Engineering
Department of Mechanical and Aerospace Engineering
Pulchowk Campus

Date: 26th November, 2023

ABSTRACT

With the development of in the field of aerodynamics, a test model of aircraft, UAVs, MAVs and other flying and moving vehicles needs to go under rigorous test in wind tunnel for stability, lift, drag and other aerodynamics parameters. Despite of development of CFD for flow simulation over a body, experimental setup with proper flow conditions is necessary for carrying out actual aerodynamics test. The study presents conceptual design, numerical simulation and experimental setup of low speed open jet wind tunnel of blower type having test section of 1.5 m in width and 0.8 m in height. The wind tunnel was able to produce 7 m/s of free jet at outlet where the test object can be placed. The flow field evaluation showed mean flow uniformity lies mostly below 5%. Experiments related to aerodynamic loading was also carried out in this wind tunnel. Similarly, control surface response of UAV was observed in this wind tunnel. The development of such open jet wind tunnel can be useful for simulation of flights and testing of aerodynamic forces in test model of aircrafts.

Keywords: Wind Tunnel, Subsonic, Open Jet, Blower Type

ACKNOWLEDGEMENT

I would to express my deepest gratitude to Department of Mechanical and Aerospace Engineering of Pulchowk Campus, IOE, Tribhuvan University for providing opportunity to explore in the field of wind tunnel. I would like to thank all the lecturers and staff of Department of Mechanical and Aerospace Engineering for their continuous support.

I would like to express my deepest appreciation to Professor Dr. Laxman Poudel and Assistant Professor Dr. Sudip Bhattrai for their supervision and guidance throughout the thesis. I am extremely grateful to respected Assistant Professor Kamal Darlami and Assistant Professor Ashish Karki for their support and valuable suggestions. I would like to thank external supervisor Ashish Manandhar for his valuable feedback.

I would like to thank Abhishek Bhandari for his support during testing of wing loading and Nabin Bhandari for his assistance during wind tunnel test of UAV. I could not have undertaken this journey without my fellow friends Akin Chettri, Salim Maharjan, Sandip Gewali, Sagar Khatiwada, Aayush Bhatta, Krishna Adhikari and Siddartha Poudel. They have been my companion in each and every step research especially during fabrication. I would like to acknowledge Pratibha Bhandari and Nischal Poudel for their support during data processing.

This endeavor would not have been possible without the support of teachers from Carpentry Section, Mechanical Workshop and Incubation, Innovation and Entrepreneurship Center (IIEC) of Pulchowk Campus. I'm extremely grateful to Chandrika Nand Adhikari and Chhedi Narayan Sharma of Mechanical Workshop and to Biscuit Maharjan of Carpentry Section for their immense support during fabrication.

Last but not the least, I would like to thank my family and my friends who were also a backbone to this research work.

TABLE OF CONTENTS

LIST OF TABLES

LIST OF FIGURES

LIST OF ABBREVIATIONS

CFD	Computational Fluid Dynamics
DMAE	Department of Mechanical and Aerospace Engineering
IIEC	Incubation, Innovation and Entrepreneurship Center
IOE	Institute of Engineering
JAXA	Japan Aerospace Exploration Agency
MAV	Micro Air Vehicles
MS	Mild Steel
NASA	National Aeronautics and Space Administration
ONERA	Office National D'études et de Recherches Aérospatiales
UAV	Unmanned Air Vehicles
USAF	United States Air Force
WOW	Wall of Wind

LIST OF SYMBOLS

%	Percentage
µ	Dynamic Viscosity of fluid
μ_i	Flow Uniformity
2-D	Two dimensional
A	Cross-sectional Area
A_1	Cross-sectional Area of Settling Chamber
A_2	Cross-sectional Area of Test Section
AR	Area ratio or Contraction Ration
D	Diameter
D_h	Hydraulic Diameter
H	Height
HP	Horsepower
km/h	Kilometer per hour
KW	Kilo Watt
KWHr	Kilowatt Hour
L	Length
L	Length of contraction
Li	Half Length of contraction
M	Mach Number
M	Meter
m/s	Meter per second
m^2	Square Meter
m^3/hr	Cubic meter per hour
m^3/min	Cubic meter per Minute
mm	Millimeter
N	Number of Samples
P	Pressure
$P_{dynamic}$	Dynamic Pressure
P_{static}	Static Pressure
P_{total}	Total Pressure

Q	Total Volumetric Flow Rate
Q'	Volumetric Flow Rate of Each Fan
Re	Reynolds Number
R_i	Half Length of inlet section
R_o	Half Length of outlet section
Rpm	Revolution per Minute
U	Velocity of Fluid
$\bar{u}$	Average Velocity
u_i	Instantaneous Velocity
V	Velocity of Fluid
V_1	Velocity at Settling Chamber
V_2	Velocity at Test Section
W	Width
W	Watt
β	Honeycomb Porosity
ρ	Density of fluid

CHAPTER ONE:
INTRODUCTION

1.1 Background

History has shown that flying has always been a challenging tasks for human. Observing the birds fly, human always wanted to take aircrafts heavier than air to make it fly and carry humans. After the successful flight by Wright brothers in the year 1903, the development of powered and controlled aircraft took a new turn. Even then, the sustained flight was a challenge. Also, human wanted to go as fast as they could. This led into development of the aerodynamics field. The shape of an aircraft plays an important role in determining how much drag an aircraft faces when it is in flight. Also, it is important to know how much lift can be created by the shape of the aircraft such that it sustains during the flight. Furthermore, it is important to observe the forces (thrust, drag, lift and weight) and pressure on the aircraft body and stability of the control system.

It important to account for responses of control surface such as horizontal and vertical stabilizers, rudder, flaps, ailerons, canard, etc. (components of an aircraft) while moving through air at different altitude, airspeed, etc. It is also necessary to observe the aerodynamic load in wings of an aircraft and observe for wing vibration. This can help to avoid resonance frequency which can cause flutter effect in wing.

Before manufacturing a full scale aircraft, it is necessary to simulate the aircraft in the similar environment. The surrounding conditions can affect the flight. In real conditions, the surrounding air is stationary and the aircraft is moving through it. But, it is very expensive and rigorous to test in such conditions (Anderson, 2017). So, the concept of wind tunnel was developed in order to experimentally verify the similar conditions present in the environment.

Wind tunnel is an experimental setup in which the controlled air stream flows through the stationary model of the designed aircraft or objects. This will help to acquire knowledge about the behavior of the aircraft in flight condition. Different research groups (such as NASA, Rolls Royce, Boeing) and universities uses wind tunnel to experiment on scale models or full prototype of aircraft and spacecraft. Wind tunnel can also be used for testing of automobiles, buildings, etc.

Different types of wind tunnel can be found according to their flow speed and their applications. Some of them are: low and high speed wind tunnel, subsonic and transonic wind tunnel, supersonic wind tunnel, hypersonic wind tunnel, high enthalpy wind tunnel, boundary layer wind tunnel, automobile wind tunnel (Anderson, 2017). Low speed wind tunnel can be further categorized into an open return tunnel and closed return tunnel. Closed return tunnel is a tunnel in which air recirculates inside a closed path whereas an open return tunnel has both ends open and draws air into the test section. There can be open or close test section where the model is exposed to desired airflow to study their performance under controlled conditions.

A type of wind tunnel that produces open free air flow to the body that is to tested for aerodynamic properties is known as open jet wind tunnel. In such wind tunnel, open test section is present at upstream of a fan/blower or compressor (Mehta & Bradshaw, 1977). Converging contraction section is generally used in this type of tunnel. As a result, higher velocities and precise measurement of aerodynamic parameters are possible as the air can be accelerated when it reaches the test area. In open jet wind tunnel, the test section is not bounded by walls having an open test section.

One of the major benefit of open jet wind tunnel is that it has open test section. It has smaller effective blockage ratio than a closed jet wind tunnel. As the airflow from the wind tunnel is not constrained by the walls, the flow is comparatively less distorted than in wind tunnel having closed test section (Grogger, et al., 2022). Also, the vibrations produced by the test object during aerodynamic loading or during movement of control surface of test model is directly dissipated into the surrounding giving an advantage of testing flying or moving objects. Also, in open test section, researcher can easily access the test model without hassle of opening and closing of observation area and carry out the experiments.

However, wind tunnel having blower/fan has some disadvantages. One of the most severe disadvantage is having inherent higher turbulence level originating from upstream fans. The flow should be made laminar as much as possible while carry out crucial tests.

1.2 Problem Statement

An open jet wind tunnel is necessary to perform free flight test of UAVs and gliders. Wind tunnel having open test section can help to access and modify the test object easily. The wind tunnel design is crucial for determining the flow inside test section. It must replicate the test conditions and velocity in which the aircraft will be flown. The design of individual component determines the flow characteristics. The desired velocity of the air must be stable in test section. Similarly, there must be flow uniformity when flow exits from outlet into the test model.

Researches has been carried out to develop such wind tunnel. Blower wind tunnels usually have centrifugal fan as drive system. Such wind tunnel contains diffuser between drive system and settling chamber which makes wind tunnel longer in length. Also, such wind tunnel is not suitable to carry out test for large test models as contraction ratio has to be maintained in order to obtain proper flow. So, a new concept has to be developed to obtain optimum flow speed and test section enough to accommodate large test objects.

1.3 Objectives

Main Objectives

- To design, fabricate and evaluate performance of a low speed open jet wind tunnel and perform a free flight test of a glider

Specific Objectives

- To evaluate design specifications of individual components of wind tunnel on the basis of size of required velocity and test section
- To perform CFD simulation to observe flow characteristics inside wind tunnel
- To fabricate the experimental setup, collect experimental data of velocity and compare with CFD simulation
- To observe aerodynamic load in wind and to perform observe control surface response of UAV in open test section

1.4 Scope of the Project

The experimental setup will contribute to the field of experimental aerodynamics. The project will accommodate the principle of continuity equation to converge the airflow. The project will account for performance evaluation through flow uniformity at outlet of wind tunnel. The flow velocity will measure with the help of anemometer. The developed setup can be used to observe aerodynamic loads in wings and conduct free flight test of gliders, UAVs, MAVs and model aircrafts. The control surface response of UAV can also be observed with the help of this wind tunnel.

1.5 Limitation of the Project

As the project is focused on developing the experimental setup of wind tunnel only, the measurement of different parameters such as forces and pressures is not possible through this setup. Further development can enclose these features.

Along with that, the honeycomb was not used in the experimental setup. Also, the wall of wind tunnel was not smooth enough due to roughness of plywood. These factors might affect the flow inside the wind tunnel.

CHAPTER TWO:
LITERATURE REVIEW

2.1 Wind Tunnel

Wind tunnel is an experimental setup for investigation of airflow on test models. In wind tunnel experiments, airflows through the test model in controlled manner. Generally, scaled version of full scale actual body is tested in wind tunnel. The interaction of prototype or model with the airflow can be characterized and behavior of model can be observed in the wind tunnel. The principle of wind tunnel is based on Continuity equation and Bernoulli theorem. Reynolds number is used as non dimensionless parameter in order to scale up/down a test model. The scaling of model is done through keeping Reynolds number constant.

2.2 History of Wind Tunnel

Wind tunnel has been developed over a period of time from 18th century. Whirling Arm apparatus was developed by Benjamin Robins in the initial phase for determining drag. Further development by Sir George Calyley (whirling arm of 5 feet and top speed of 3 to 6 m/s) was used to measure lift and rag of various airfoil.

Experiments by the Englishman Osborne Reynolds in 19th century showed that pattern of airflow in both scale model and full model would have similar pattern, if certain parameters were identical. Reynolds number is now used as basic parameter to describe fluid flow situations for flow patterns, heat transfer and turbulence.

in 1901, Wright brothers developed a wind tunnel which assisted them to investigate on the effects of airflow over different profiles during the development of Wright Flyer.

In 1909, Gustave Eiffel developed first open-return type wind tunnel. The wind tunnel was powered by a 67 HP (50KW) motor. The wind tunnel was useful to set new benchmark for aeronautical research. This wind tunnel with test section of two-meter is still operational today in Auteuli, France. This wind tunnel was significantly improved by Eiffel through addition of test section in chamber, honeycomb straightener with flared inlet and diffuser between fan and test section.

During 19th century, the wind tunnel was required in the field of aerodynamics and aeronautical engineering. Different wind tunnels can be found developed over this period of time. The US Navy built 7 feet diameter wind tunnel with the help of electric motor with paddle type fan blades with power rating of 500HP. The Chalais-Meudon wind tunnel (S1Ch by ONERA) was used to develop the Concorde and the Caravelle. Similarly, in a conversation held between General Arnold and von Kármán in 1939 about requirement to advance USAF, von Kármán suggested that the first step was to construct the right wind tunnel. Many wind tunnels were developed during and after World War II. The wind tunnel in NASA, JAXA, ONERA, etc. has the facility to test full scale model. Figure 1 shows the testing of aircraft model in the wind tunnel present at NASA.

Figure 1 Testing of Aircraft in Wind Tunnel at NASA (May, 2015)

Computational Fluid Dynamics can act as supplement or possibly replace the wind tunnel experiments for limited applications. For instance, the design of SpaceShipOne (an experimental rocket plane) was without the application of wind tunnel. However, to refine computational model, a flight test was carried out attaching flight threads on wind surface during an actual flight. Due to limitations of present day computing resources, CFD is not practical for flow having external turbulent flow. It is complex for to use CFD to study the flow effects around bridges, terrain and structures.

Low speed wind tunnel can be seen developed in order to test characteristics of flow around test model at subsonic speed. Low speed wind tunnel works at very low Mach number (M<0.4, ~134m/s, 480 km/h). Subsonic wind tunnel can be Eiffel type (open-return type) or Prandtl type (closed return type) where a large axial fan is used as drive system to overcome losses due to viscous effect and increase dynamic pressure.

2.3 Mathematical Basis

As mentioned above, the wind tunnel works on principle of continuity equation and Bernoulli's equation.

Continuity equation states that the product of velocity of fluid and cross-sectional area is constant at any given point. This equation can further be described as conservation of mass.

If A represents cross-sectional area and V represents velocity of the fluid, then, mathematically, from continuity equation:

$$AV = constant \qquad \text{Eq.1}$$

$$\frac{dA}{A} = -\frac{dV}{V} \qquad \text{Eq.2}$$

Bernoulli's equation gives the relation between velocity and pressure for inviscid and incompressible flow (Anderson, 2017). If p is pressure, ρ is density and V is velocity of fluid, then from Bernoulli's equation can be stated as:

$$p + \frac{1}{2}\rho V^2 = constant \qquad \text{Eq.3}$$

$$P_{total} = P_{static} + P_{dynamic} = P_s + \frac{1}{2}\rho V^2 \qquad \text{Eq.4}$$

The contraction ratio of the wind tunnel can be defined as the area ratio of settling chamber and test section. The contraction ratio or area ratio can mathematically be written as:

$$AR = \frac{A_1}{A_2} \qquad \text{Eq.5}$$

where, A_1 = Area of settling chamber

A_2 = Area of test section

Along with these principle, Reynolds number is also used to determine the flow characteristics as well as to scale the test model changing some parameters. Reynolds number helps to find out either the flow is steady, turbulent or transitional. Reynolds number is a non dimensionless parameter which can be defined as the ratio of inertial forces to viscous force in a fluid flow. The flow is said to laminar if Re<2000, turbulent Re>4000 and transitional if Re lies between 2000 and 4000 (Anderson, 2017).

Mathematically, Reynolds number can be written as:

$$Re = \frac{\rho U L}{\mu} \qquad \text{Eq.6}$$

Where,

ρ = Density of fluid,

L = Characteristic length,

U = Velocity of fluid flow and

μ = Dynamic Viscosity of fluid

The Reynolds number is used to determine the flow characteristics at the outlet.

2.4 Available Wind Tunnel

Various wind tunnels are available around the world to study the flow characteristics around the test object. Table 1 shows researches carried out to build low speed wind tunnel with open jet test section.

Table 1 Previous researches on Open Jet Wind Tunnel

S. No.	**Wind Tunnel Name**	**Application**	**Location**	**Test Section**	**Flow Velocity (m/s)**	**References**
1	Subsonic Open Jet Wind Tunnel	Educational tool for undergraduate instruction	Virginia, US	0.7m*0.7m	30	(Borgoltz, 2018)
2	Blower Wind Tunnel	Aerodynamic Research	Diyala, Iraq	0.5m*0.5m*1m	20	(Azzawi, 2023)
3	Blower Type Wind Tunnel	Educational Use	Budapest, Hungary	0.35m*0.35m, 0.4*0.5m and 0.15*1m	24 19.5 15	(Gulyás & Balczó, 2014)
4	Bird Flight Experiment Wind Tunnel	Bird Flight Research	Austria	2.5m*1.5m	16	(Grogger, et al., 2022)
5	Open Jet Wind Tunnel	Outdoor Pool Fire Experiment	Anhui, China	23m*9m	14.34	(Lei, et al., 2021)
6	Open Jet Wind Tunnel	Quadcopter Flight Testing	Malaysia	2m(D)	8	(Jurij, et al., 2019)
7	Wall of Wind	Hurricane Wind and Rain impact	Florida, USA	6m*4.3m	70m/s	(Chowdhury, et al., 2017)

2.5 Previous Works

Various wind tunnel has been developed over the course of time for the study of the aerodynamics property of the aircraft. Virginia Tech has an open circuit blower type facility as subsonic open jet wind tunnel (Borgoltz, 2018). The wind tunnel comprised of steel frame as stable base, aluminum composite panels and extruded aluminum frame for light weight strong structure. A 30HP BC-SW Sized Twin City centrifugal fan is used as drive system capable of producing $15m^3/s$ of volumetric flow. The wind tunnel consists of diffuser, settling chamber, contraction nozzle and test section as described in design by (Mehta & Bradshaw, 1977). The centrifugal fan is connected to a diffuser of length 4m at an angle of 6^o. The airstream then enters into settling chamber of width 1.78m and height 1.47m. The settling chamber consisted of honeycomb of cell size 0.01m and length 0.09m. Three screens made up of 0.3mm diameter fiberglass and open area ratio of 55% is used for turbulence reduction making flow uniform. The contraction nozzle used in this wind tunnel is defined by polynomial profile of 5^{th} degree. The flow from the wind tunnel exits at 30m/s into test chamber of 0.7m from contraction nozzle having contraction ratio of 5.5:1.

(Azzawi, 2023) has designed and characterized a new subsonic blower type wind tunnel having test section of 0.5m by 0.5m. This paper presented the employment of a large scale CFD model of whole wind tunnel in design process and evaluated pressure losses during wind tunnel operation and then used these pressure losses to determine the power required during operation of tunnel. The wind tunnel was simulated using “Intake Fan” boundary condition at inlet and atmospheric pressure at outlet. The wind tunnel was driven by a centrifugal fan of 5.5KW having backward facing aerofoil type blades. The airflow of $6.25m^3/s$ from the wind tunnel entered into 33.4^o diffuser maintained at area ratio of 3:1. Screens having porosity of 0.67 was used in diffuser. After that, the flow entered into settling chamber where honeycomb of 100mm thickness and three mesh screens were placed. Then, the flow was converged using contraction section having area ratio of 7.8:1 over the length of 160cm. This paper also presents the measurement of flow uniformity and turbulence intensity with the help of Pitot-static tube and hot wire anemometer in the empty test section. The wind tunnel can be operated at stationary speed range of 2m/s to 20m/s changing the frequency from 5Hz to 45Hz with the help of variable frequency diver.

The study by (Gulyás & Balczó, 2014) at Theodore von Kármán Wind Tunnel Laboratory presents development of blower type wind tunnel having interchangeable test sections. The wind tunnel was driven by a 4.8KW centrifugal fan having flow rate of $3m^3/s$. The wind tunnel consisted of wide angle diffuser at angle of 40^o in order to make flow uniform. To avoid separation, flat split diffuser was used. The settling chamber of 1m*1m consisted of a honeycomb and three screens. The contraction was designed using 3^{rd} degree polynomial equation suggested by (Wattmuff, 1986). The wind tunnel was able to produce 24 m/s from contraction of 0.35m*0.35m*1m designated as "high-speed". Another 2D contraction of 0.15m*1m*1m was able to produce 19.5m/s and the "wide" contraction of 0.5m*0.4m*1 was able to produce 15m/s. Through flow field evaluation in test section, the turbulence intensity was found to be 0.8% and inhomogeneity in flow was below 3%.

Another research by (Grogger, et al., 2022) developed a low cost wind tunnel to carry out experiment about bird flights. They developed a blower type wind tunnel to test the flight during ascent and gliding for Northern Bald Ibis. This wind tunnel had free jet test section with 2.5m*1.5m cross-sectional area and maximum speed of 16m/s. Figure 2 shows the scale and components of wind tunnel developed for the bird flight experiment. The wind tunnel used eight ventilator fans having volumetric flow rate of 26920 m^3/hr in each fans. They estimated the pressure losses in every section. The fan was introduced to rectangular inlet, then to big concave converging nozzle and small convex converging nozzle. The air then exited through the outlet where the birds were placed. Total power consumed by these fans was 32 kW. This paper also presented the flow quality inside the wind tunnel and the turbulence intensity present at different velocity in distance of 0m, 1m and 2m away from the outlet.

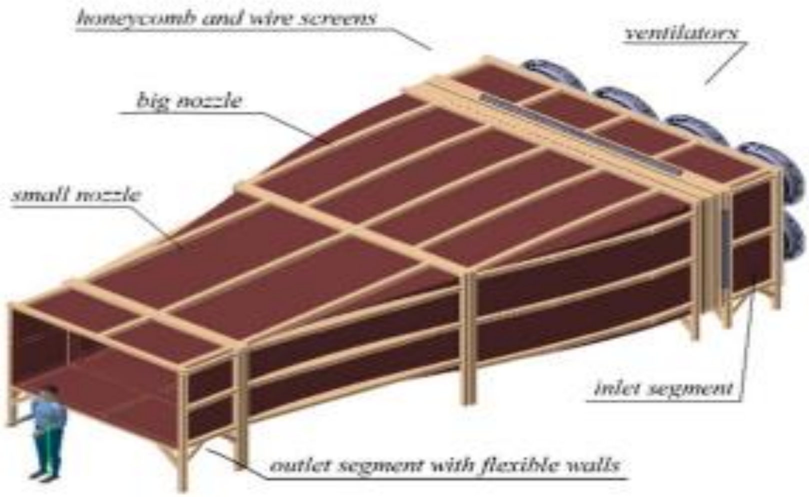

Figure 2 Full Wind Tunnel (Grogger, et al., 2022)

The research by (Jurij, et al., 2019) presented about development process and testing of wind tunnel of open jet type to test the flight quadrotor in . They used fan from the current open loop wind tunnel present at their Aerodynamics Laboratory. The extended diffuser of 2.3m diameter was used where the quadrotor could be tested. The flow from fan with diameter 1.4m was diverged into 2.3m test section. There was settling chamber were honeycomb with wire mesh was present. This wind tunnel could produce maximum of 8m/s of wind. The velocity distribution was observed at four different distance from opening with the help of anemometer. The wind tunnel had the turbulence intensity of around 20%.

A large scale experimentation facility was developed to study the impacts of hurricane wind and rain in infrastructures and buildings (Chowdhury, et al., 2017). This was Wall of Wind(WOW) at Florida International University. Different layout structures of fan were studied and CFD simulation was carried out using OpenFOAM. The WOW was powered using 12 fans (each fan having 522kW producing 111m^3/s airflow) arranged in six fans in two rows. The wind tunnel was capable of producing 70m/s of wind and Hurricane of Category 5 in Saffir-Simpson Scale.

The wind tunnel present at Department of Mechanical and Aerospace engineering in the IOE Pulchowk was also studied. This tunnel can be used for force measurement and flow visualization of the aerodynamic surfaces. In this wind tunnel, the nominal speed can reach upto 12 m/s. The test section available is of 250 mm x 250 mm x 1050 mm. (AeroStream, 2017) This wind tunnel used 16 vacuum motor for suction of air. Figure 3 shows the current wind tunnel available at IOE Pulchowk.

Figure 3 Wind Tunnel at IOE Pulchowk (AeroStream, 2017)

Along with these study, basic design were studied about wind tunnel running at low speed (Barlow, Rae, & Pope, 1999). Different power considerations, power losses, test flow quality, etc. were studied and implied in the research. Design rules were further studied from researches done by (Mehta & Bradshaw, 1977). They mentioned about the overall design procedure of the low speed wind tunnel in which blower is used as drive system. (Mehta & Bradshaw, 1977) mentioned about the design factors such as inlet conditions, screen positioning, wall shape, screen shape, drive system, contraction ratio should be considered to design the wind tunnel.

Similarly, (Chanetz, et al., 2020) mentioned about the usefulness of wind tunnel in the field of aerodynamic design. The experimental approach for flight test and necessity of wind tunnel is discussed in this book. Different wind tunnel can be used as per requirement and suitable visualization technique such as surface flow visualization, visualization by optical imaging, Schilieren and Shadowgraph can be used. Along with that, measurement of aerodynamic forces and moments with the help of aerodynamic balances such as strain and force gauges, balance of ground vehicle, sting type force balance could be used.

The study was carried also out to study low speed wind tunnel that could produce unsteady flow. Wind tunnel developed by (Greenblatt, 2016) was of blowdown type in which longitudinal freestream oscillation can be produced with the help of linearized governing equations.

CHAPTER THREE:
RESEARCH METHODOLOGY

3.1 Methodological Flowchart

The overall design procedure followed to carry out study of low speed open jet wind tunnel is shown in the Figure 4.

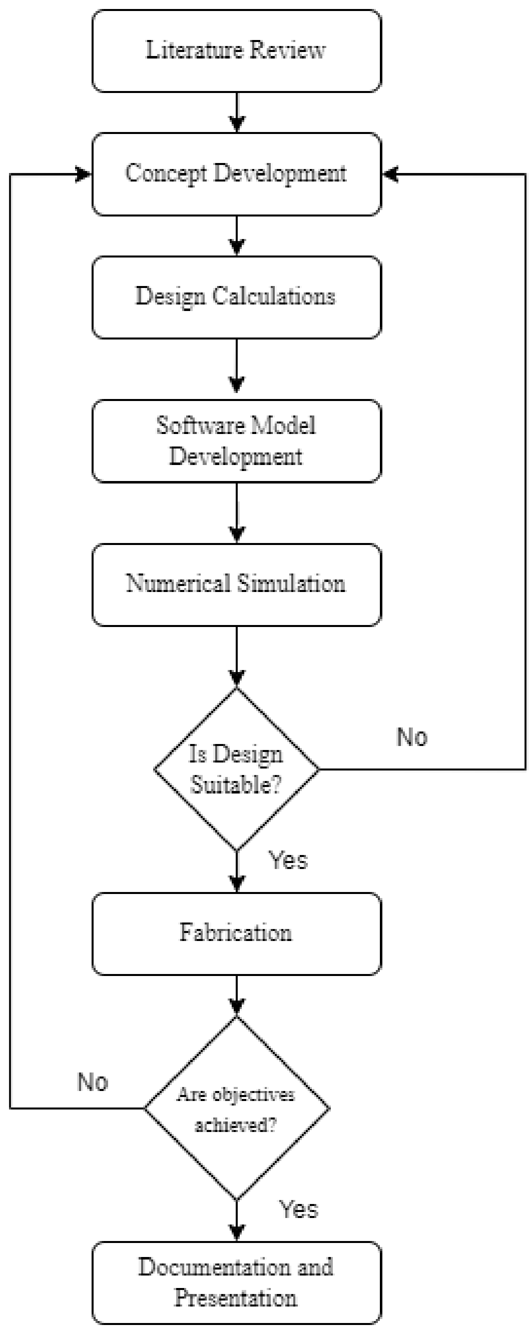

Figure 4 Methodological Flowchart

The above flowchart shows the study of different literature in order to develop concept, perform calculations, make CAD models and simulate and eventually check design criteria. After successful simulation, the design model is then fabricated and experimental data are taken for performance evaluation.

3.2 Literature Review

Literature review was done with the help of different reference books, journal articles and previous researches carried out by different researchers The research works in the field of experimental aerodynamics and in wind tunnel was studied. The information is being gathered from the journal related to aerodynamics, fluid mechanics, ornithology, wind engineering, etc. The focus of these studies was to study the necessary flow conditions, how the setup was developed and necessary analysis to be done for study of flow characteristics.

3.3 Concept Development

The primary design concept was developed through comparative study of different previous researches carried out to study wind tunnel. Overlooking the advantages and ease of access to test models, a wind tunnel having open jet was necessary to carry out free flight tests. Preliminary concept was to have a square or circular test sections. However, upon exploring the types of glider and UAVs, it was found that they have long wing span. Thus, to include whole structure of the model, outlet exit was designed to have rectangular test section. Similarly, to ease the fabrication process, 2-D contraction design provided by Wattmuff (Wattmuff, 1986) was selected. Anemometer available in the department was selected as tool for performance evaluation.

3.4 Design and Calculations of Open Jet Wind Tunnel

The main factors considered for the design of this wind tunnel are outlet cross-section and flow velocity at outlet. The required length of outlet cross section is selected as 1.5m considering the length of wind span, blockage ratio and the height of available gliders and UAVs. Similarly, the required velocity at exit to open test section is considered to be 12 m/s. The design of each component of the wind tunnel are based on these considerations.

3.4.1 Outlet

Based on above length of exit of wind tunnel, the suitable width was selected as 0.8m (just more than half of length). The outlet area is given by:

$$A_2 = 1.5m * 0.8m$$

$$A_2 = 1.2m^2$$

Thus, area of the outlet was evaluated as 1.2m^2. Also, for length of outlet section, half of hydraulic diameter was taken. The considered length helps to make the flow uniform after contraction and minimize flow losses.

$$Dh_{outlet} = \frac{2ab}{a+b} \qquad \text{Eq.7}$$

$$Dh_{outlet} = \frac{2*1.5*0.8}{1.5+0.8}$$

$$Dh_{outlet} = 1.04m$$

Thus, the length of outlet is considered as 0.52m.

3.4.2 Drive System

Blower/fan is selected as the drive system of the wind tunnel. The drive system should be able to produce volumetric flow rate which can create 12m/s airspeed in outlet area of 1.2m^2. The required volumetric flow rate is given by:

$$Q = A * V = 1.2m^2 * 12m/s = 14.4m^3/s \qquad \text{Eq.8}$$

$$Q = 51840m^3/hr$$

In order to obtain such large flow rate, a single fan with very large diameter is required. It is very expensive to purchase a single fan with such huge flow rate. So, for achieving the required flow rate, multiple fans are arranged in array such that the flow rates of individual fan are combined. Flow rates of fans are combined when they are arranged in parallel. Such arrangement can be seen in wind tunnel for bird flight experiments (Grogger, et al., 2022) and Wall of Wind at Florida International University (Chowdhury, et al., 2017).

Taking consideration of losses in different components, overall required flow rate is considered as 54000 m^3/hr. Upon researching on market about available fans, farrata fans were found suitable and affordable. Each 20 inches farrata fan is capable of producing the flow rate of 5400m^3/hr.

So, number of fans required to produce the flow rate is given by:

$$N = \frac{Q}{Q'} = \frac{54000}{5400} = 10 \qquad \text{Eq.9}$$

The flow velocity that can be obtained using this drive system is given by:

$$V_2 = \frac{N*Q'}{3600*A_2} = \frac{10*5400}{3600*1.2} = 12.5m/s \qquad \text{Eq.10}$$

The above equation is derived through continuity equation $A_1V_1 = A_2V_2$. The left side of this continuity equation shows the total available volumetric flow rate at inlet. Thus, the velocity of 12.5m/s can be produced using these fans.

Table 2 Fan Description

Company	CG
Model	CGFFA030
Power Rating	130W
Motor Speed	1400 rpm
Number of Fans	6
Company	Usha
Model	Farrata EX
Power Rating	160W
Motor Speed	1400 rpm
Number of Fans	4
Air Delivery	90m^3/min (5400m^3/hr)
Size	20inches (500mm)

Table 2 Fan Description shows the description of the fans used to make the wind tunnel. At first, it was decided to used CG farrata fan as it met the design criteria and was affordable. However, due to unavailability of remaining CG fan, four Usha fan having similar air delivery were used.

Total power consumed by the drive system is 1420W. This means that these fans will consume 1.42 KWHr (1.42 units) of electricity if the continuous testing for one hour.

3.4.3 Inlet

The dimension of the inlet section was evaluated on the basis of fan diameter. As mentioned in table, each farrata fan has the diameter of 20 inches. Considering the frame size, each fan occupied 22 inches. To accommodate fans in matrix of 5x2 and avoid touching with each other, a space of 116 inches in width and 45 inches in height is required. The dimension of inlet was considered as 2.95m by 1.15m. The inlet has 10 holes of 20.5inches to let the airflow from the drive system to enter into the wind tunnel.

The inlet area is given by:

$$A_1 = 2.95m * 1.15m = 3.3925m^2$$

Area Ratio

The area ratio is given by:

$$AR = \frac{A_1}{A_2} = \frac{3.3925}{1.2} = 2.827$$

3.4.4 Settling Chamber

The inlet section is connected to the settling chamber where the flow settles. The width and height of the settling chamber is same as the inlet i.e. 2.95 in width and 1.15 in height. The length of settling chamber is taken as half the hydraulic diameter is order to minimize the flow losses. The evaluated length of settling chamber is 0.85m.

Usually settling chamber consist of flow conditioner such as honeycomb and wire screens. Honeycomb is used in settling chamber to make flow laminar as much as possible. The design of the honeycomb is based on criteria that honeycomb porosity (β) should be more than 0.8 and length-hydraulic diameter ratio should be between 6 to 8. The design procedure of honeycomb is mentioned in (Teseletso, Namoshe, Subaschandar, & Kutua, 2015). Figure 5 shows the discretion of honeycomb as designed in Table 3 Description of Honeycomb

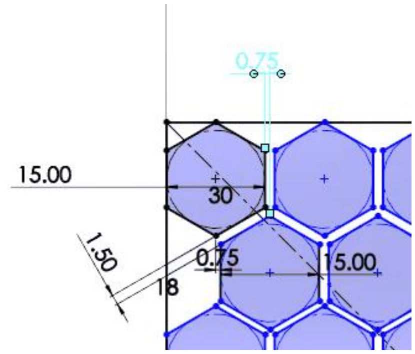

Figure 5 Description of Honeycomb

Table 3 presents the description of the designed honeycomb. Based on this calculation, total of 9897 honeycombs would be required to meet the flow criteria.

Table 3 Description of Honeycomb

Description	**Symbol**	**Calculated**	**Unit**
Cell diameter	dhoney	15	mm
Sheet Thickness	Shoney	0.75	mm
Length	Lh	100	mm
Honeycomb Cell Side length	lhoney	8.66	mm
External Cell Side	Lg honey	9.52	mm
Division	Zhoney	36.37	
Honeycomb Porosity	Beta	0.91	
Cell Hydraulic Diameter	Dh	15.75	mm
Length-hydraulic Diameter ratio	Lh/Dh	6.34	

Figure 7 shows the honeycomb structure in 500mm by 500mm structure. From the calculations, it was found the honeycomb with 15mm diameter was suitable enough to provide porosity of 0.91. Along with that, the length to hydraulic diameter ratio was maintained at 6.34.

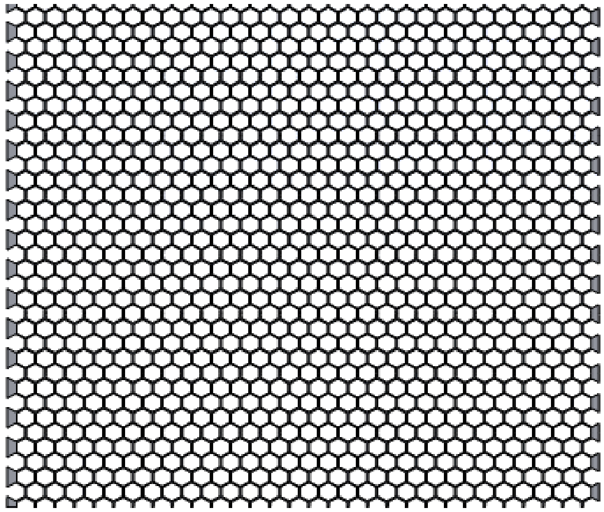

Figure 6 Honeycomb structure

Along with the honeycomb, wire screens of different mesh sizes are used. Wire screens help to reduce the large eddy from the fans into smaller one. The smaller eddy loses energy and dissipates while travelling inside the wind tunnel.

3.4.5 Contraction

The design of contraction is selected carefully to avoid flow separation at inlet and exit of contraction. The proper design of wind tunnel helps to reduce losses due to formation of Gortler vortices. Different equations were studied for designing the contraction curve. Wattmuff (Wattmuff, 1986) studied the effect of contraction profile on pressure gradient at inlet and outlet. He suggested that contraction profile joined by two third degree polynomial equation joined by inflection point sufficiently minimizes pressure gradient at the inlet. This helps to avoid boundary layer separation in contraction profile. So, the contraction profile suggested by Watmuff was used to design the wind tunnel. The polynomial equations of the contraction profile are:

$$R_1(x) = R_i - A_1 x^n \quad and \quad R_2(x) = R_o + A_2(L-x)^n \qquad \text{Eq.11}$$

$$L_i = 0.5L \quad and \quad A_1 = A_2 = \frac{R_i - R_0}{2L_i^3} \qquad \text{Eq.12}$$

Where,

R_1, R_2 = equation of for concave profile and convex profile

R_i, R_o = half-length of inlet and outlet section (1.475m and 0.75m respectively)

L = length of contraction(L=Dh=1.7m)

L_i = inflection point (0.5L=0.85m)

The final equation can be written as

$$R_1(x) = 1.475 - 0.59x^3 \qquad \text{Eq.13}$$

And $$R_2(x) = 0.75 + 0.59(1.7 - x)^3 \qquad \text{Eq.14}$$

The Equation 13 and Equation 14 are implemented to define concave and convex profile of sidewalls from the top view. Also, the top and bottom part is decreased form 1.15m to 0.8m with an inclination angle of 5.8^o. As the flow is converging and the inclination angle is very less compared to overall size of wind tunnel, there is minimal chances of flow separation in the contraction section due to this slope. The overall dimension of each component of the designed wind tunnel is mentioned in Table 4.

Table 4 Dimension of each component of Wind Tunnel

Components	**Dimension**
Fan Inlet	0.52m(D)
Inlet	2.95m(W)*1.15m(H)
Settling Chamber	0.85m(L)*2.95m(W)*1.15m(H)
Contraction Length	1.7m
Outlet	0.52(L)*1.5m(W)*0.8m(H)

3.5 Software Model Development

The software model was developed using CAD software called Solidworks. The overall design of the wind tunnel can be seen in the following figure. Similarly, a fluid domain was created in order to simulate the flow inside the wind tunnel. The flow entered the domain through 10 inlets of size 20.5 inches (520mm). In order to make simulation more realistic, the inlet was made 50mm inside the wind tunnel.

Figure 7 represents the overall structure created in CAD software. The wind tunnel contains settling chamber, contraction section and outlet.

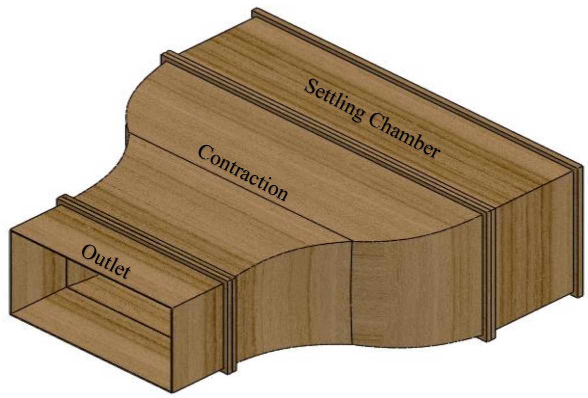

Figure 7 Overall CAD model of wind tunnel

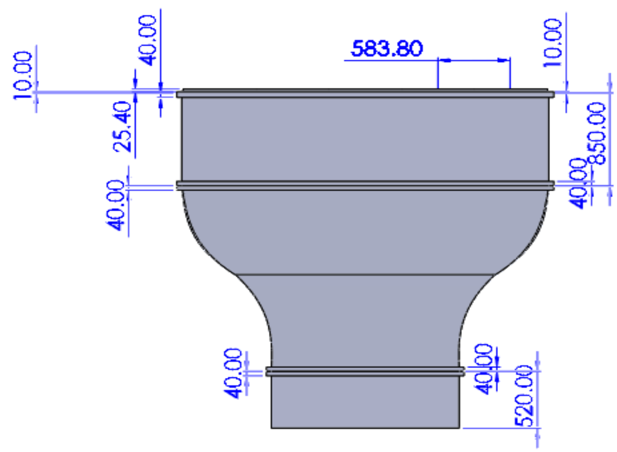

Figure 8 Wind Tunnel Top View

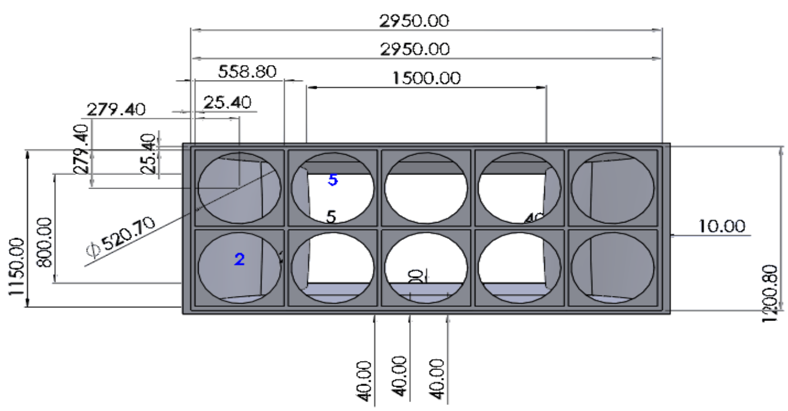

Figure 9 Wind Tunnel Back View

Figure 8 and Figure 9 represents the top view and back view respectively along with the dimensions of the wind tunnel.

3.6 Numerical Simulation

The numerical simulation was carried out in CFD software called ANSYS. The fluid domain made in Solidworks was imported to ANSYS and simulations were performed in different boundary conditions.

3.6.1 Meshing

Mesh independence was done by varying different mesh sizes and mesh quality. The fluid domain was then discretized into tetrahedral mesh of element size 20mm. The number of nodes were 361399 and number of elements were 1966986.

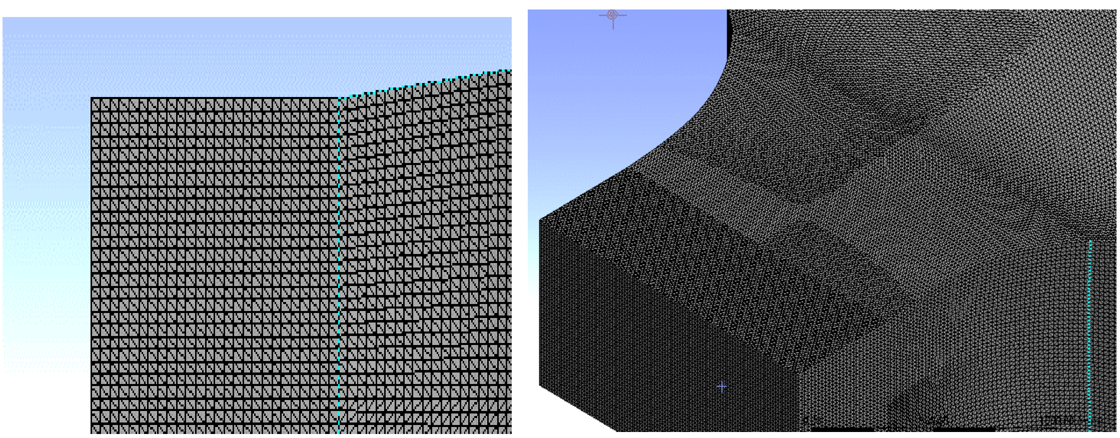

Figure 10 Tetrahedral Mesh of Wind Tunnel

3.6.2 Setup for Simulation

To carry out simulation of subsonic flow in fluid domain inside the wind tunnel, k-ε realizable turbulence modelling was considered. The inlet boundary condition was considered as mass flow inlet considering volumetric flow rate of 54000 m^3/hr i.e. ρAV = 18.375 kg/s. The density of air was considered as 1.225 kg/m^3. The other boundary conditions are shown in Table 5.

Table 5 Boundary Conditions

Model	k-ε model, Realizable
Inlet	Mass Flow Inlet 18.375 kg/s
Outlet	Outflow
Method	SIMPLEC
Scheme	Second Order Upwind

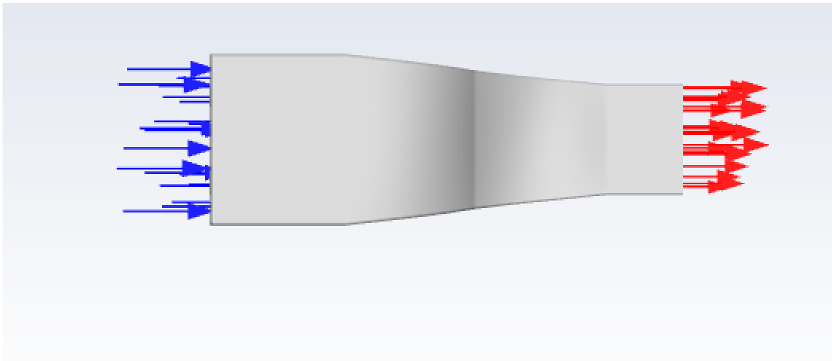

Figure 11 Boundary Conditions applied

Figure 11 shows the flow direction of the flow from inlet and outlet in which boundary conditions are applied.

3.6.3 Simulation Results

Velocity and Pressure contour were obtained from the simulation. These plot shows that velocity of 12.3 m/s can be obtained at outlet.

Velocity plot

Contour of velocity magnitude were obtained from the simulation. Figure 12 shows the velocity that can be obtained at the outlet. Another plot in the mid plane represents the mixing of flow from inlet and obtaining a uniform velocity at the outlet.

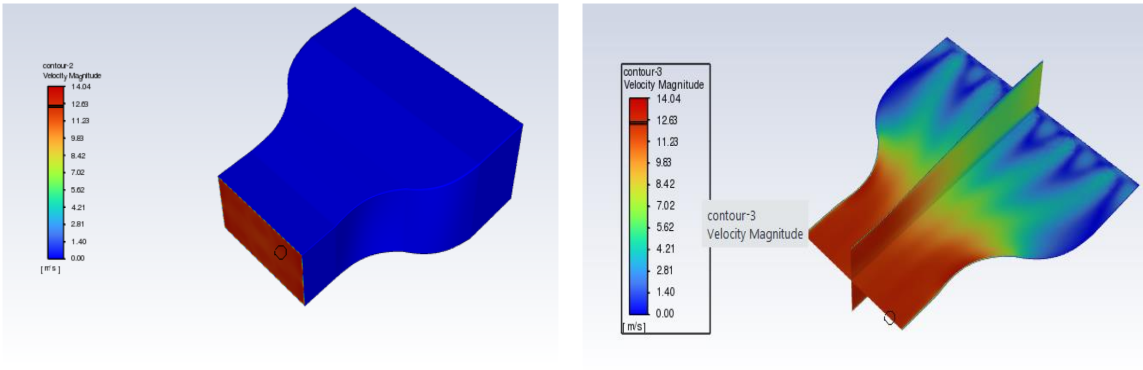

(a) (b)

Figure 12 (a) Velocity Contour at outlet (b) Velocity distribution in Mid plane

Figure 13 and Figure 14shows the variation of velocity at outlet along X-axis and Y-axis respectively. Velocity above 12 m/s can be obtained in both directions in outlet.

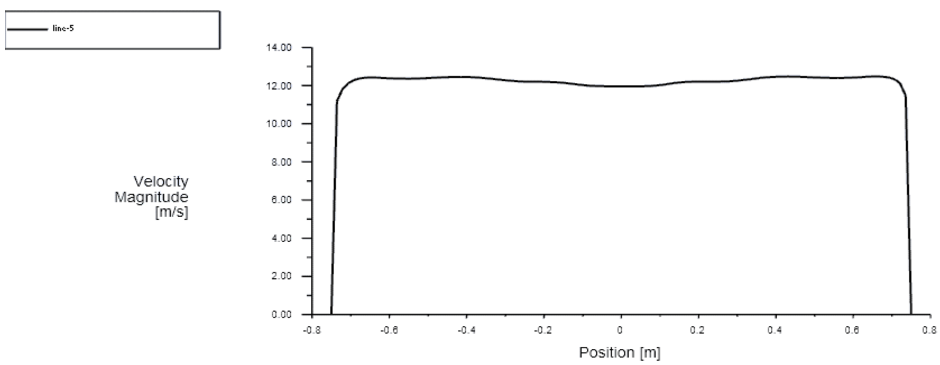

Figure 13 Velocity in Outlet along centerline in X axis

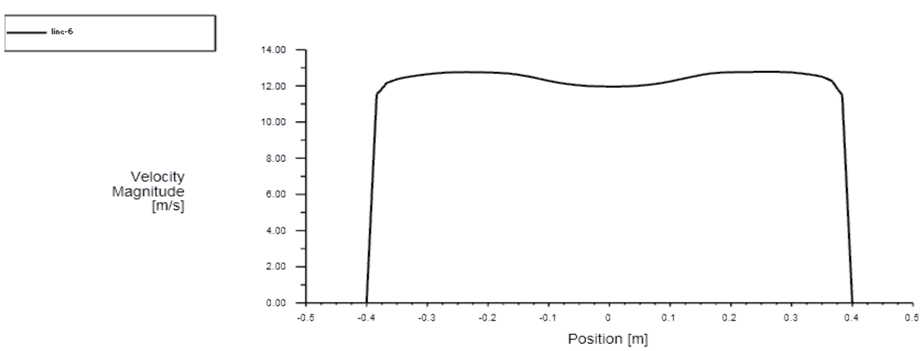

Figure 14 Velocity at outlet along centerline in Y-axis

Figure 13 represents the velocity along the centerline in Z-axis. It can be observed that the velocity increases gradually along the centerline and reaches upto 12.3 m/s at outlet.

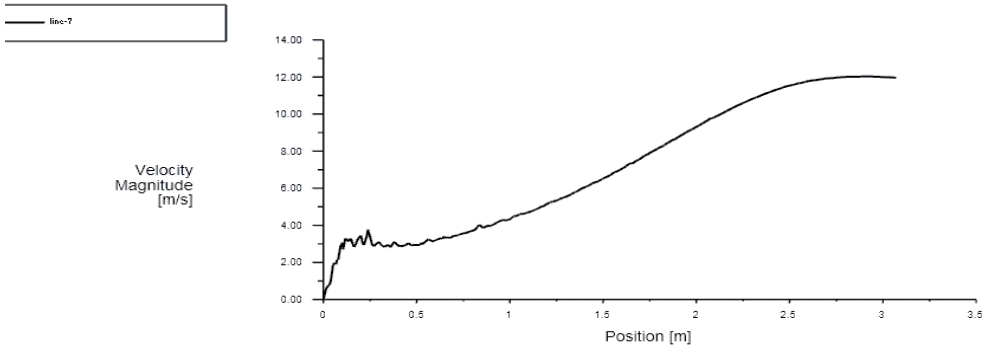

Figure 15 Velocity Plot along centerline in Z axis

Pressure Plot

Plots were obtained for static pressure, dynamic pressure and total pressure. Figure 16 represents the static pressure. From the plot of static pressure, it can be observed that the static pressure rises initially due to intermixing of flow and decreases when it reaches to contraction section. The static pressure reaches to -68.2 Pa when it reaches at outlet.

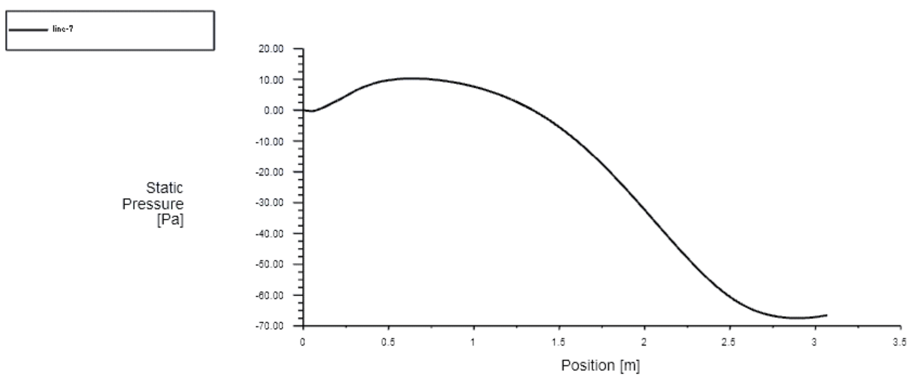

Figure 16 Static Pressure along Centerline

Figure 17 represents dynamic pressure along the centerline. Dynamic pressure increases slowly in the settling chamber and increases along with length in contraction and outlet. The dynamic pressure rises up to 88 Pa at the outlet.

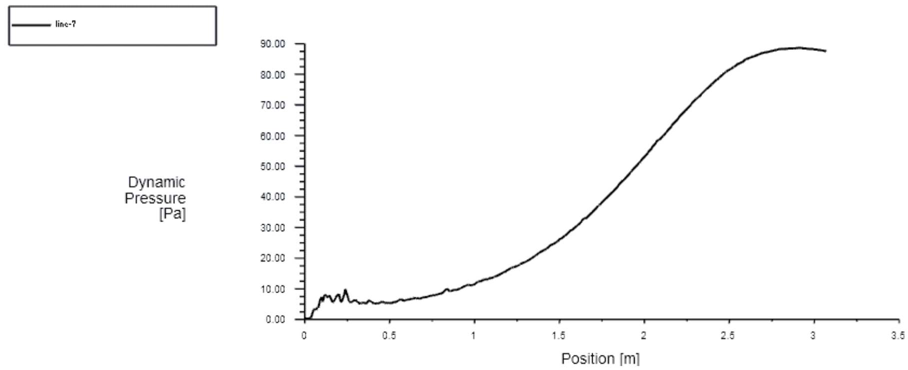

Figure 17 Dynamic Pressure along Centerline

3.7 Fabrication

3.7.1 Table Top Model

Before making a full scale model, a table top model was fabricated on the basis of geometric similarity. The table top model was built in the ratio of 1:10. The objective of making this model was to learn about the manufacturing process and use of laser cutting of plywood. This table top model helped in visualization of how final model is going to look like physically.

In case of table top model, the size of inlet section was determined by available fans. Two fans of 120 mm size were used to make the model. The description of the table top model is mentioned in the Table 6.

Table 6 Details of Table Top model

Components	**Description**
Inlet	240mm*120mm
Drive System	Two fans of 120mm size Inlet Velocity = 3m/s
Outlet Section	150mm*80mm Type: Open Jet
Area Ratio	2.4

The design and dimensions of table top model are presented in figures below.

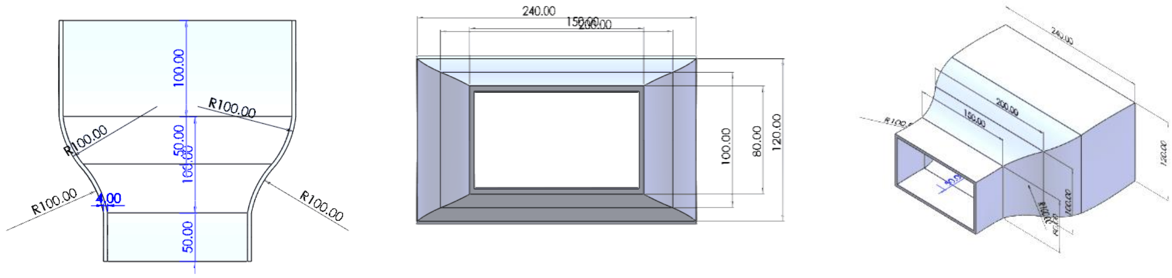

Figure 18 Different views of Table Top Model

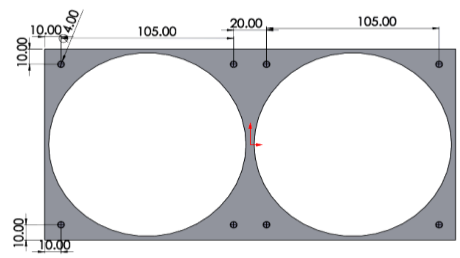

Figure 19 Fan Inlet of Table Top Model

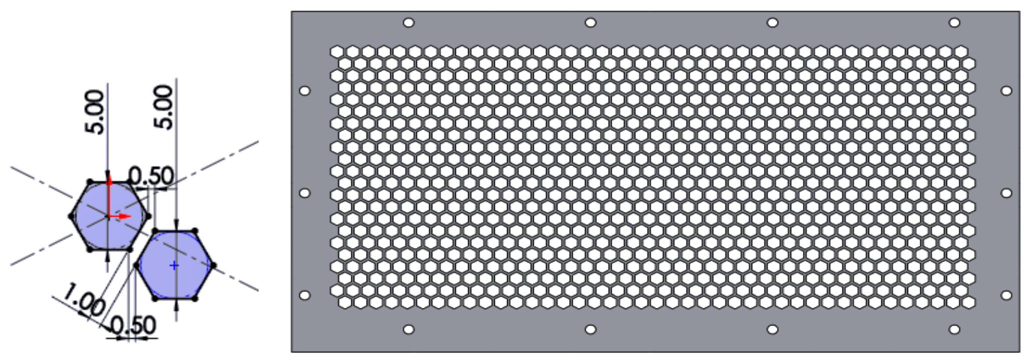

Figure 20 Honeycomb Structure

The table top model was fabricated using 5mm plywood. Flexible plywood was used to make the contraction section. The fabricated model is shown in the figure below:

(a) (b)

Figure 21 (a) Fan used in Table Top Model (b) Placement of Honeycomb

Figure 22 Overall Structure of Table Top Model of Wind Tunnel

The fabricated table top model was able to produce an airstream of 4.5-5m/s. The velocity was less compared to simulation. This might have been caused due to rough surface of plywood and uneven surface created during manufacturing. Avoidance of these errors can help to obtain required velocity and flow quality.

3.7.2 Full Scale Model

After learning and visualization from the table top model, the full scale model was fabricated in the carpentry section of Pulchowk Campus. To hold all fans, metal structure of 2 inch heavy MS square Pipe was used as fan stand. The stand was able to hold fans in matrix of 5*2. This metal stand was then connected to a frame structure made up of 1inch square pipe having 22inch space in middle to accommodate whole structure of fan. The frame was taken as fan inlet. Circular hole of 20.5 inch was cut using laser cutting machine available at Manufacturing Lab of DMAE. Further, the contraction curve was cut in the plywood through the same laser cutting machine. Settling chamber, contraction section and outlet section were then fabricated and assembled together.

(a)

(b)

(c)

(d)

(e) (f)

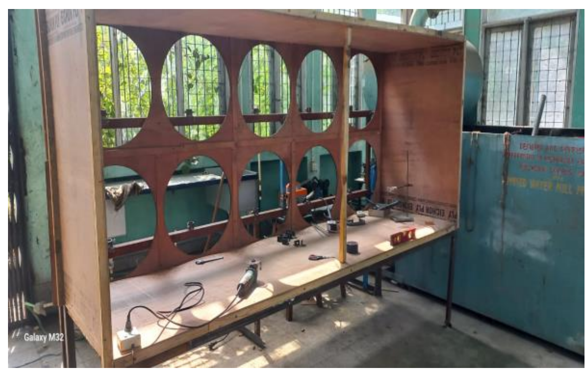

(g) (h)

(i) (j)

(k)

Figure 23 Fabrication Process of Wind Tunnel

Description of each figure:

- Figure 23(a) represents fan stand to hold all 10 fans and inlet to make airflow inside wind tunnel.
- Figure 23(b) represents outlet section of 1.5m*0.8m.
- Figure 23(c) represents settling chamber of 2.95m*1.15m.
- Figure 23(d) represents assembly of contraction section and outlet section.
- Figure 23(e) represents assembly of settling chamber, contraction and outlet section.
- Figure 23(f) represents complete assembly of wind tunnel
- Figure 23(g) represents final fan stand along with frame to hold settling chamber in IIEC.
- Figure 23(h) represents placement of settling chamber.
- Figure 23(i) represents placement of all fans in fan stand.
- Figure 23(j) represents placement of fine mesh.
- Figure 23(k) represents overall final structure of wind tunnel.

The final assembly of the wind tunnel was placed in IIEC Pulchowk.

3.8 Performance Evaluation

The validation is done through comparison the experimental results with the result form the CFD simulation. The experimental data was taken with the help of anemometer. Data were taken from inside the wind tunnel, at outlet and away from the outlet. The variation of velocity in different location were plotted in MATLAB.

The evaluation of the velocity distribution in the outlet plane was carried out. The outlet plane was divided into 0.1m*0.1m square pockets as shown in Figure 24. There were 15 sample pockets horizontally and 8 sample pockets vertically making total of 120 sample points.

Figure 24 Division of Outlet Plane

The velocities from each sample points were collected and flow uniformity was observed. The flow uniformity (μ_i) can be evaluated through:

$$\mu_i = \frac{u_i - \bar{u}}{\bar{u}} \ \ and \ \ \bar{u} = \frac{1}{N}\sum_{i=1} u_i \qquad \text{Eq.15}$$

Where, u_i = instantaneous velocity

$\bar{u}$ = average velocity

N = number of samples = 120

The plots showing performance is described in results and discussion section.

3.9 Documentation of Findings and Presentation

Documentation of finding and presentation of the results is carried out on the basis of the guidelines provided by the Department of Mechanical and Aerospace Engineering. These obtained results is then submitted to the Department after the approvals from the supervisors.

CHAPTER FOUR:
RESULTS AND DISCUSSION

4.1 Experimental Data

4.1.1 Velocity at different speeds

Data were collected from outlet in the sample points as mentioned in methodology. The data obtained at different speeds of fan is mentioned in the following sections. Attention was given while taking data to study the wind tunnel characteristics in free stream. The flow from the wind tunnel must not have any blockage and flow must move freely into the surrounding. The experimental data obtained from anemometer is mentioned in APPENDIX B: EXPERIMENTAL DATA Equation 15 was used to determine the flow uniformity.

Fan Speed Low

All ten fans were set in low speed and the data were recorded with the help of anemometer. The average velocity obtained at this speed of fan was 5.62 m/s. The velocity fluctuations were almost within the limits of 5%.

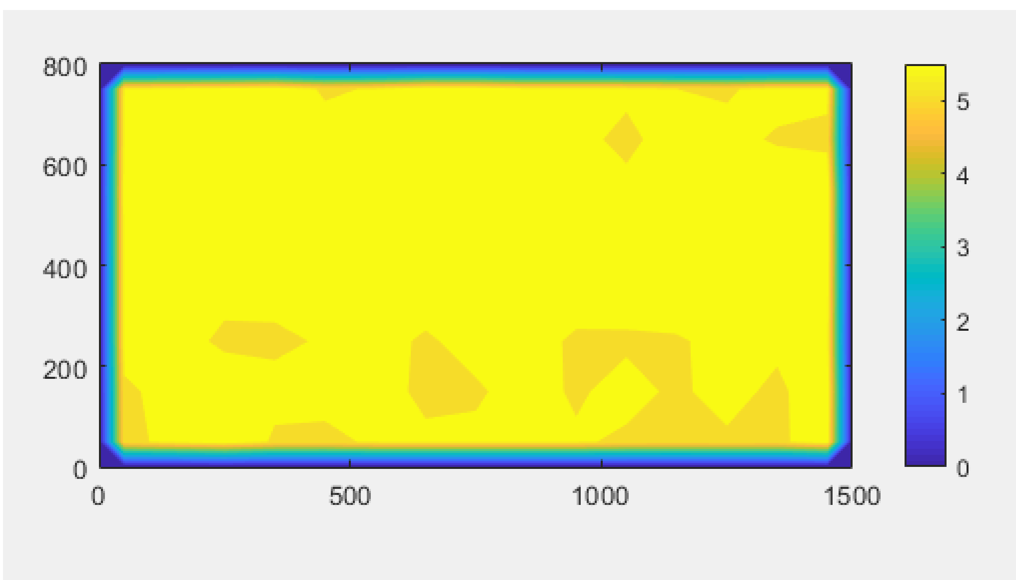

Figure 25 Velocity at Low Speed

It can be observed in Figure 25 the data that flow fluctuates in near wall reasons. This is due to boundary layer formation in wall regions.

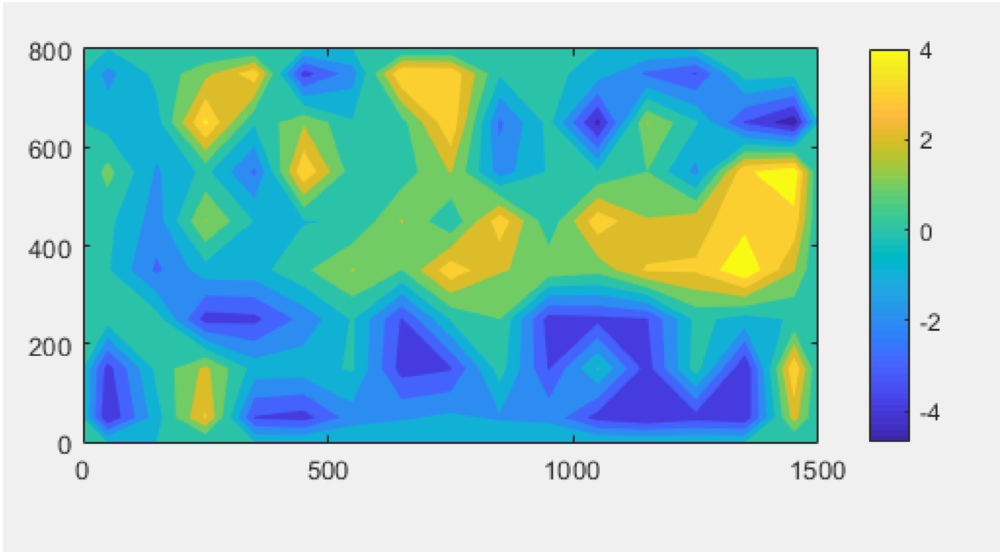

Figure 26 Flow Uniformity at Low Speed

From flow uniformity plot in Figure 26, it can be seen that the flow fluctuates +4% to -4% from average. This fluctuation can be seen due to swirl component coming from fan. The flow is turbulent due to this reason.

Fan Speed Medium

After that, all ten fans were set in medium speed and the data were recorded with the help of anemometer. The average velocity obtained at this speed of fan was 5.97 m/s. From the flow velocity plot in Figure 27, it can be observed that the flow velocity is fluctuating. In some regions, flow can flow is above 6m/s.

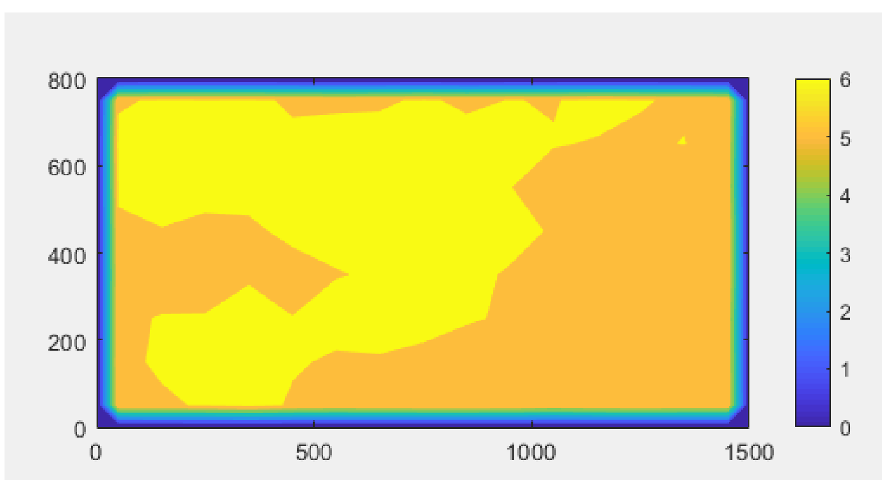

Figure 27 Flow Velocity at Medium Speed

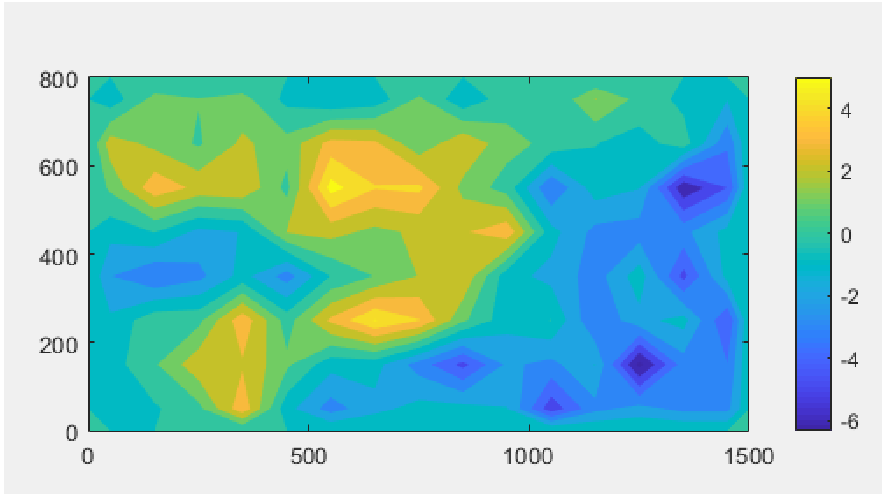

Figure 28 Flow Uniformity at Medium Speed

Figure 28 shows the flow uniformity plot in fan speed II. It can be observed that flow uniformity parameter fluctuates between -6% to +4% from the average. Also, it can be noticed that the flow uniformity decreases when the speed increases.

Fan Speed High

After that, all ten fans were set in high speed and the data were recorded with the help of anemometer. The average velocity obtained at this speed of fan was 6.3 m/s. However, in some region, the maximum velocity was 6.65m/s. From the velocity contour in Figure 29, it can be seen that velocity is above 6 m/s in most of the regions.

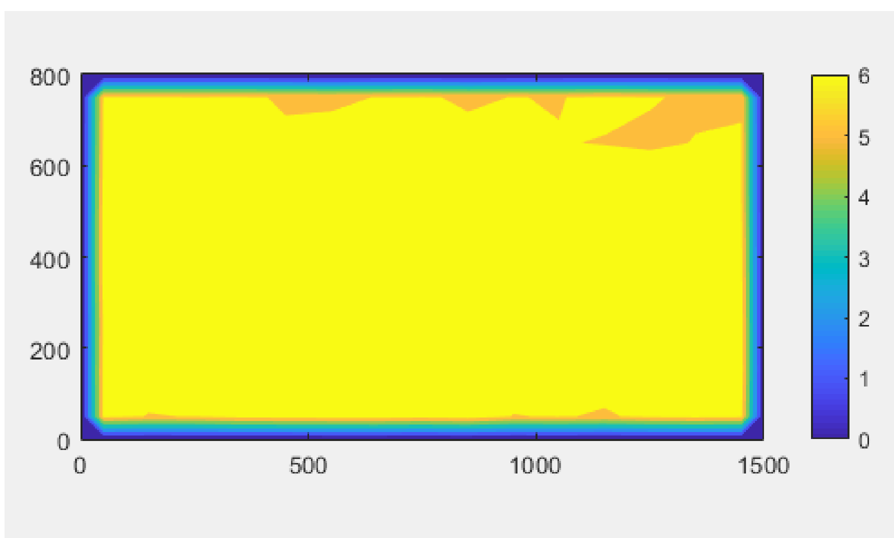

Figure 29 Flow Velocity at High Speed

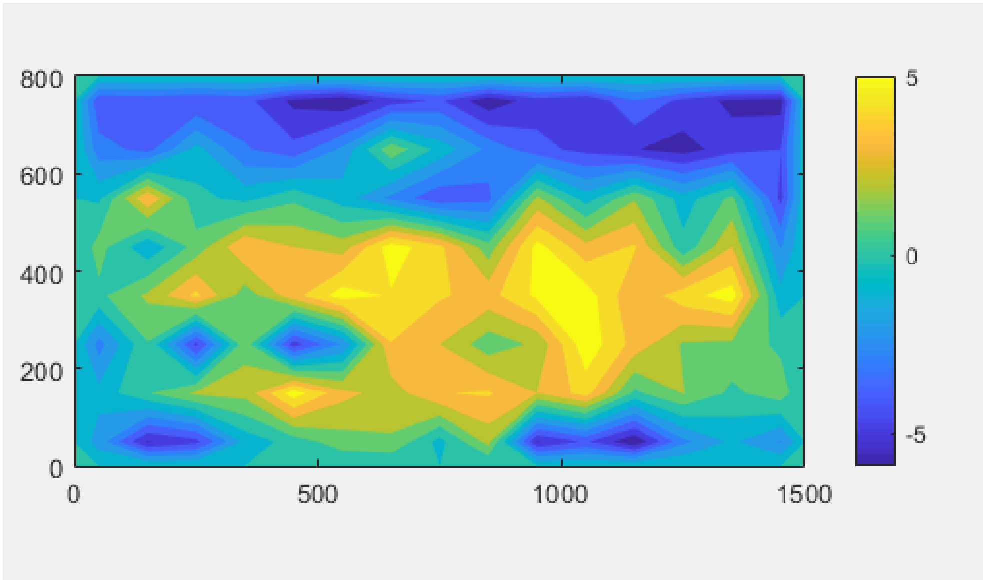

Figure 30 Flow Uniformity at High Speed

From the flow uniformity plot in Figure 30, it can be observed that flow uniformity fluctuates from -5% to +5%. It can be noticed that flow velocity in center is above average in right section.

4.1.2 Velocity inside wind tunnel

The velocity along the centerline was measured along the centerline inside the wind tunnel. The Table 7 shows the variation of velocity inside the wind tunnel.

Table 7 Variation of Velocity inside the wind tunnel

Location	Velocity
Fan Inlet	3.8
Contraction Start	3.4
Contraction End	5.9
Outlet	6.65

Plot in Figure 31 shows the variation of velocity inside the wind tunnel. When the wind tunnel is running at full speed, it can be observed that the velocity from decreases to 3.8 m/s. This might be due to the back pressure created inside the wind tunnel. It further decreases up to 3.4m/s when the contraction starts. This is due to presence of fine wire screen. Then, inside the contraction section the flow from each fan intermixes with each other resulting in velocity of 5.4m/s at the contraction end. The velocity increases up to 6.65m/s when it exits from the outlet.

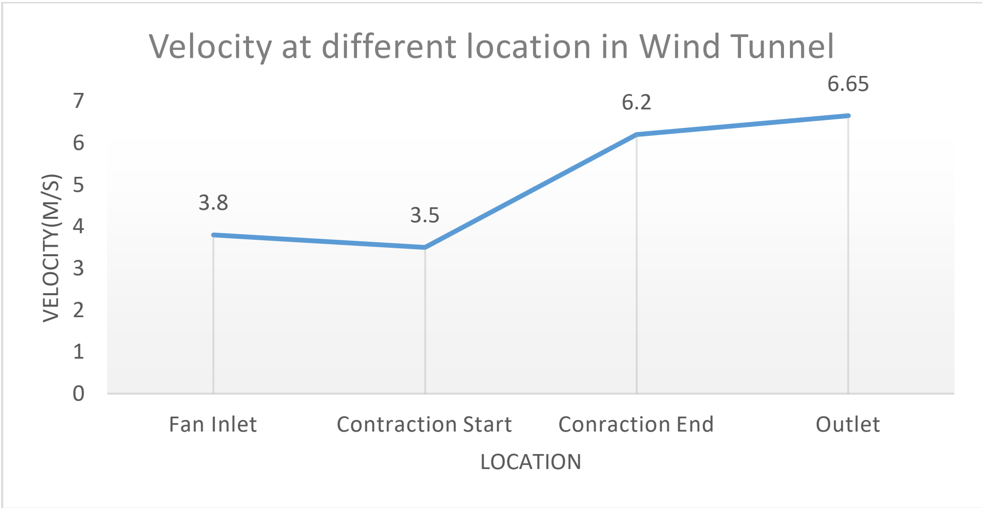

Figure 31 Plot showing variation of velocity inside wind tunnel

4.1.3 Velocity outside wind tunnel

Figure 32 shows the variation of velocity away from the outlet. The plot shows that the velocity outside the wind tunnel decreases. This is caused due to boundary layer mixing with the atmospheric air. There is 17% decrease in velocity along the span of 1.5m.

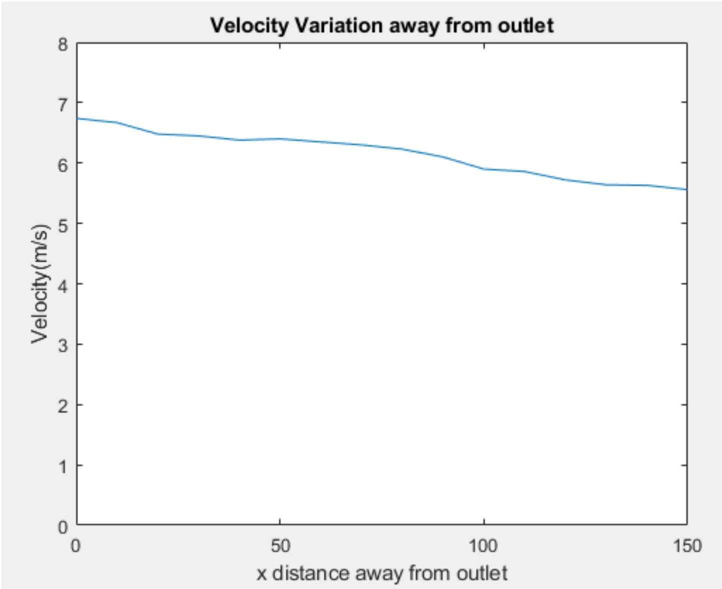

Figure 32 Velocity Variation away from outlet

4.1.4 Velocity along Centerline at outlet

Figure 33 represents the variation of velocity along the centerline at outlet in x axis and y axis respectively. From the graphs, it can be observed that the variation of velocity pattern is similar to that of variation of velocity at outlet in simulation. However, the magnitude is comparatively less in the experiment.

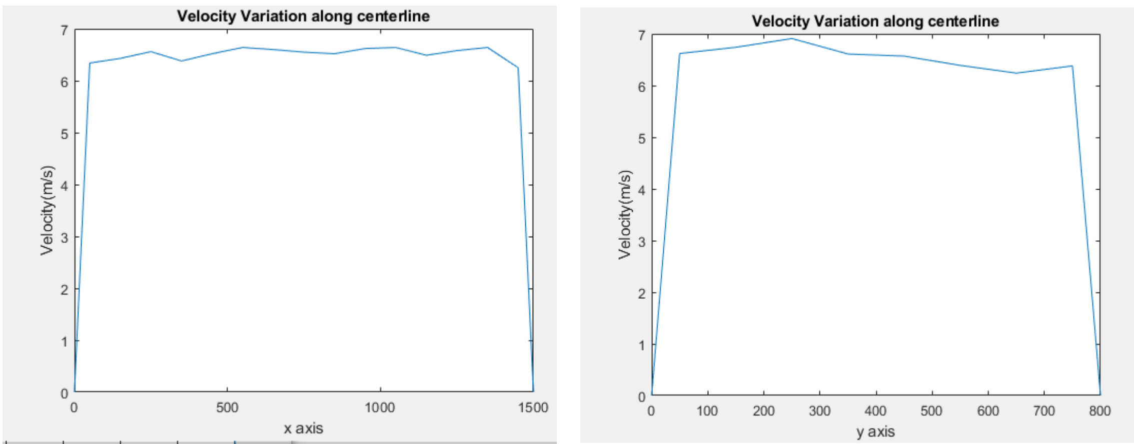

Figure 33 Variation of Velocity along Centerline in X axis and Y axis

4.2 Experiments Performed

4.2.1 Wing Loading at 18% load

The wing profile of Eppler 205 was tested for aerodynamic loading. The setup for aerodynamic loading test can be observed in Figure 34. The flow velocity of 6.5m/s was capable of producing approximately 18% of total load of 14.53N in the wing. With the help of high speed camera, the videos were taken and analyzed in MATLAB. The modal frequency with aerodynamic loading in wind tunnel was found to be 14.84 Hz. Comparing with natural frequency of wing at no load condition (15.83 Hz), the natural frequency was found to be decreased in loading condition. Further the wing was tested by changing the angle of attacks to 5^{o} and 10^{o}.

Figure 34 Setup to test Aerodynamic Loading

4.2.2 Control Surface Response

A 0.6 times scaled down model of Skywalker X8 Blended wing body UAV was used for control surface resopnse test. A setup was made with the bearing and stand to study the control surface response. The specification of the UAV is mentioned in Table 8.

Table 8 Specification of 0.6 times scaled Skywalker X8

Features	**Description**
Wingspan	1.2m
Weight	1kg
Location of CG	18cm from nose
Control surface size	40cm*5cm
Max. deflection of elevons	30 degrees

Figure 35 shows the setup and placement of the UAV in the wind tunnel. In BWB, elevons acts as control surface. During the response test, both stabilized as well as manual modes were used: Stabilized mode for the first 5 seconds and manual mode for the next 8 seconds.

Pixhawk-4 was used as a flight controller and pitot tube for measuring the airspeed of the wind tunnel in a real-time frame.

Figure 35 Setup to observe control surface response

The data obtained from the control surface response test was extracted from Pixhawk and was plotted with the help of MATLAB. Different graphs were obtained for variation of roll, pitch and yaw with time. Along with that, plots were obtained to observe airspeed, actuator control and actuator output during the flight test.

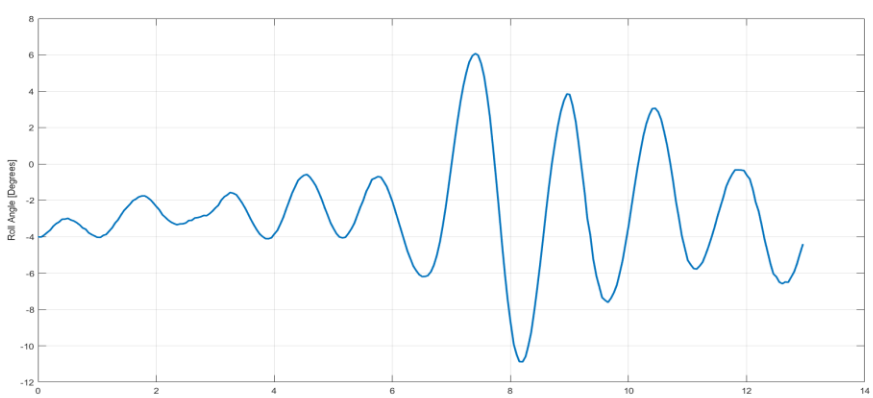

Figure 36 Plot of Roll angle vs Time

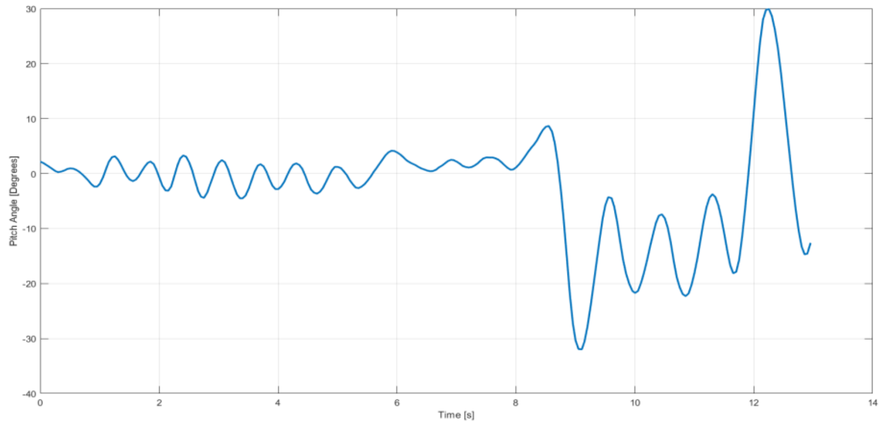

Figure 37 Plot of Pitch angle vs Time

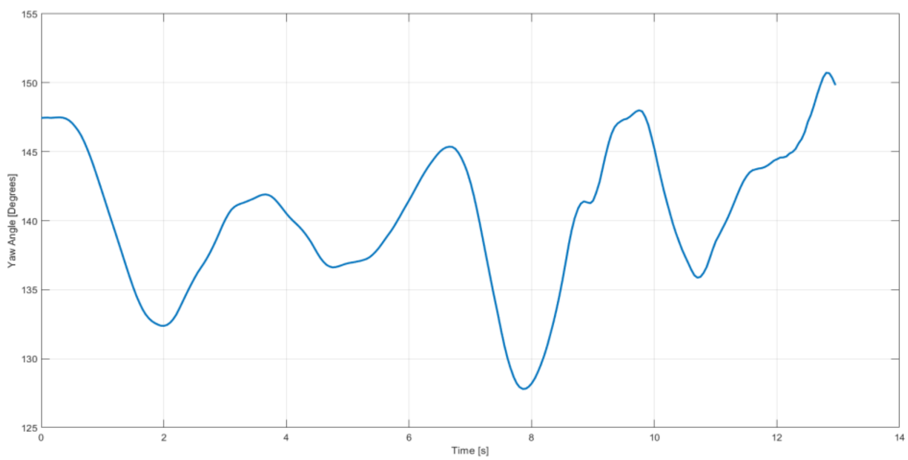

Figure 38 Plot of Yaw angle vs Time

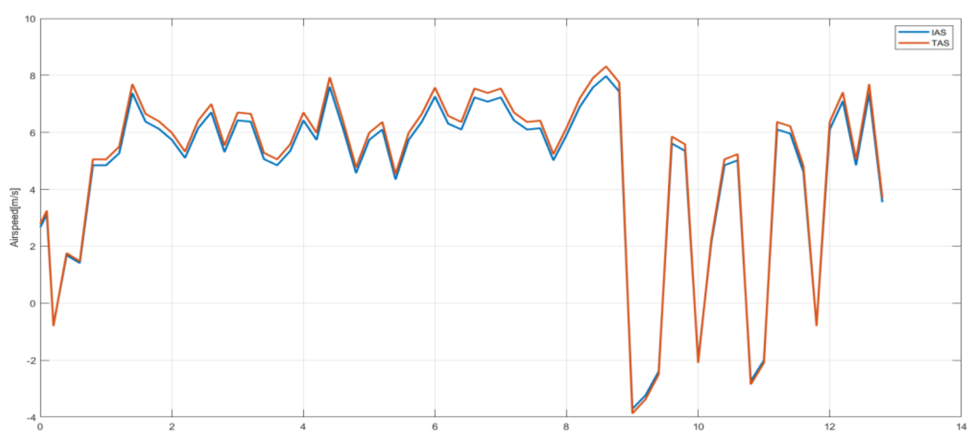

Figure 39 Plot of Indicated Airspeed and True Airspeed

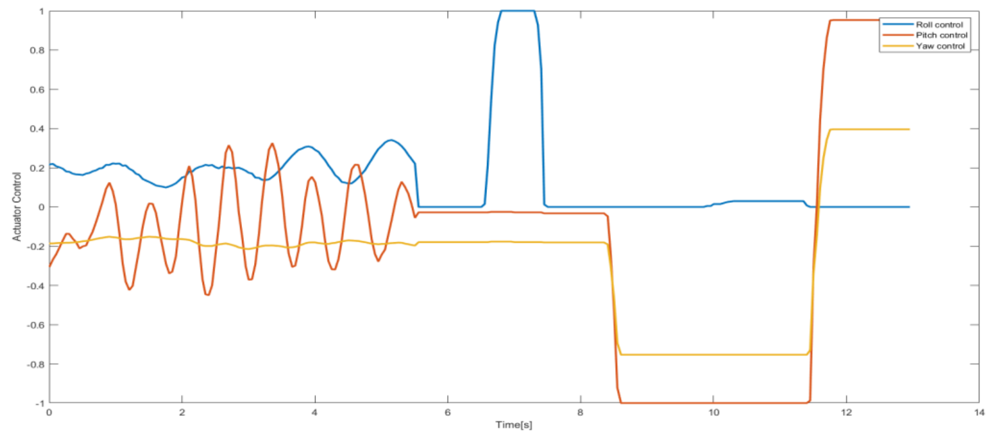

Figure 40 Plot of Roll control, Pitch Control and Yaw Control

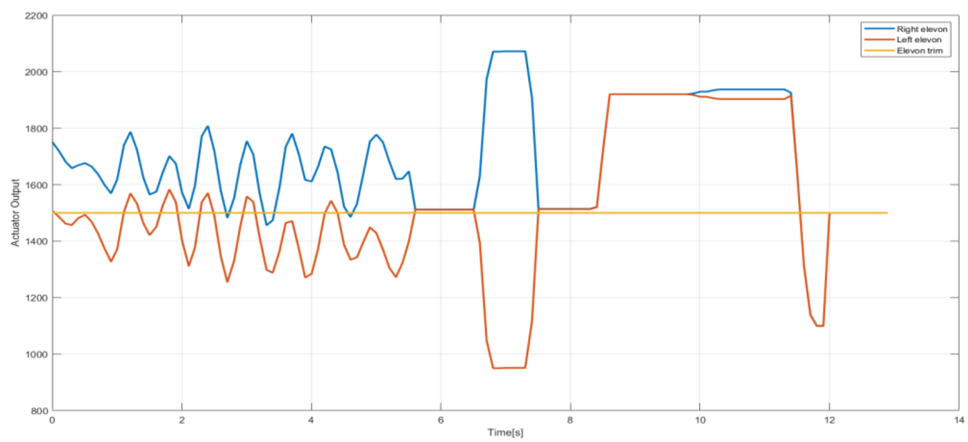

Figure 41 Plot of Actual Movement of Elevons

This UAV consists of two elevons as a control surface. Initially, the UAV was in stabilized mode. Since the wind tunnel was blowing air at the speed of 6.5 m/s, the control surfaces were automatically moved by the flight controller to maintain its level. Minimum trim, initial trim, and final trim parameters for elevons were set to 900, 1500, and 2100 respectively.

During the stabilized mode, initially when the wind tunnel was turned on UAV showed left roll behavior with a roll angle of 4 degrees, and to compensate for that behavior right elevon and left elevon were deflected at maximum and minimum 1800, 1480, and 1280, 1580 respectively. The right elevon was deflected more positively to maintain level flight. Since this aircraft consists of elevons only, while controlling the rolling moment, some sort of pitching moment and yawing moment were also observed. During this moment pitch angle varied between -2 to 3 degrees. The initial heading of the aircraft was 147 degrees and due to the yawing moment, it changed to 137 degrees.

After the completion of the stabilized mode, the manual mode was triggered with the help of a radio transmitter and the control surfaces were deflected to create roll and pitch moments respectively. At the 6th second, actuators were deflected in opposite directions, whose actuator output was 2100, 900. This actuator output created a positive roll of 6 degrees. Similarly, after testing the rolling moment in manual mode, the pitching moment was also tested. For the Pitching moment, actuators were deflected in the same direction, whose actuator output was 1930, 1920. This actuator output created a pitching moment of negative 32 degrees.

Airspeed was measured using a digital airspeed sensor called pitot tube which measures the difference between static pressure and dynamic pressure and converts to airspeed reading. During the later phase of the manual test, fluctuation in airspeed data was observed due to sudden changes in pitch and roll.

CHAPTER FIVE:
CONCLUSION AND RECOMMENDATIONS

5.1 Conclusion

In conclusion, an open jet wind tunnel was designed, simulated and fabricated. The wind tunnel can be used to test various test models of UAVs and wind profiles. The airflow inside the wind tunnel was comparatively uniform having fluctuation of flow quality of 5%.

The wind tunnel was designed to obtain 12.5 m/s. However, only 6.5m/s was obtained experimentally. This drop in velocity might be due to non-uniformity of plywood inside the wind tunnel. The decrease in velocity might be due to turbulent flow produced by fans.

The CFD simulation showed that the velocity of 12.3 m/s can be obtained inside the inside the wind tunnel.

Aerodynamic loading in wing profile of Epler 205 was observed with the help of this wind tunnel. Along with that, control surface response was observed in 0.6 scaled down model of Skywalker X8.

5.2 Recommendations

- Further improvement can help to make the flow laminar with the help of honeycomb and screens.
- Improvement can be done to improve surface inside the wind tunnel. This might decrease boundary layer and improve flow velocity and flow uniformity.
- With the help of turn table, load cells and model support pitch mechanism, different aerodynamic parameters such as lift and drag can be measured.
- Use of more powerful fans and study of flow characteristics by varying length can help to meet the requirement of the desired velocity.
- Further improvement can be done through implementation of 3D contraction design for rectangular wind tunnel.

REFERENCES

AeroStream. (2017). *Subsonic Wind-Tunnel Facility (LST-1@DME), IOE Nepal*. Retrieved from DMAE IOE: http://mech.pcampus.edu.np/our-research/our-research-dme-reseach-facilities/subsonic-wind-tunnel-facility-ioe-nepal/

Anderson, J. (2017). *Fundamentals of Aerodynamics.* New York: Mc Graw Hill Education.

Apte, V., Green, A., & Kent, J. (1991). Pool Fire Plume Flow In A Large-scale Wind Tunnel. *Fire Safety Science*, 425-434.

Azzawi, I. (2023). Design and characterizing of blower wind tunnel using experimental and numerical simulation. *Proceedings of the Institution of Mechanical Engineers Part G Journal of Aerospace Engineering*, (pp. 1-15).

Barlow, J. B., Rae, W. H., & Pope, A. (1999). *Low-Speed Wind Tunnel Testing.* New York: John Wiley & Sons, INC.

Borgoltz, A. (2018, 08 30). *0.7m subsonic open jet wind tunnel*. Retrieved from Virginia Tech University: https://www.aoe.vt.edu/research/facilities/openjet.html

Chanetz, B., Délery, J., Gilliéron, P., Gnemmi, P., Gowree, E. R., & Perrier, P. (2020). *Experimental Aerodynamics.* Switzerland: Springer.

Chowdhury, G., Zisis, I., Irwin, P., Bitsuamlak, G., Pinelli, J., Hajra, B., & Moravej, M. (2017). Large-Scale Experimentation Using the 12-Fan Wall of Wind to Assess and Mitigate Hurricane Wind and Rain Impacts on Buildings and Infrastructure Systems. *Journal of Structural Engineering*.

Greenblatt, D. (2016). Unsteady Low Speed Wind Tunnels. *AIAA Journal*, 1817-1830.

Grogger, H. A., Gossar, M., Makovec, M., Fritz, J., Neugebauer, K., Amann, F., & Voelkl, B. (2022). A low-cost wind tunnel for bird fight experiments. *Journal of Ornithology*, 599-610.

Gulyás, A., & Balczó, M. (2014). Development of a small blower-type wind tunnel for educational purposes. *28th microCAD international multidisciplinary scientific conference*, (pp. 04-10).

Hernández, M. A., López, A. I., Jarzabek, A. A., Perales, J. M., Wu, Y., & Xiaoxiao, S. (2013). *Wind Tunnel Designs and Their Diverse Engineering Applications.* IntechOpen.

Jurij, M., Nor, E., Shakrine, A., Rafie, M., Marzuki, O. F., Saad, M., & Azrad, S. (2019). Development and Testing of Open-Jet Wind Tunnel for Quadrotor Flight Testing. *Journal of Advanced Research in Fluid Mechanics and Thermal Sciences*, 304-315.

Lei, J., Huang, P., Zhang, L., Yuan, Y., Deng, W., Mao, S., & Zhang, J. (2021). Experimental study on flow characteristics of a large-scale open jet wind tunnel for outdoor pool fire research. *Journal of Wind Engineering and Industrial Aerodynamics*.

May, S. (2015, July 22). *Wind Tunnel*. Retrieved from NASA: https://www.nasa.gov/general/wind-tunnel/

Mehta, R. D., & Bradshaw, P. (1977). Design rules for small low speed wind tunnels . *Aeronautical Journal*.

Teseletso, A. T., Namoshe, M., Subaschandar, N., & Kutua, S. (2015). Design of an Open-circuit Subsonic Wind Tunnel for Educational Purpose. *Botswana Institution of Engineers (BIE) 14th Biennial Conference.* Botswana.

Wattmuff, J. H. (1986). Wind Tunnel Contraction Design. *9th Australian Fluid Mechanics Conference*, (pp. 472-475). Auckland.

APPENDIX A:

BUDGET

S. No.	Components	Expenditure
1	Fan	75000
2	Plywood	30000
3	Supporting Wood	6000
4	Supporting Frame	20000
5	Fevicol	600
6	Nails and Screw	500
7	Nut Bolts and Thread Screw	3000
8	Wire Screen	1500
9	Small Scale Model	3000
10	Transportation	4000
11	Labour Charge	6000
12	Miscellaneous	5000
	Total	154600

APPENDIX B:

EXPERIMENTAL DATA

Table 9 Data for Low Speed

	0	50	150	250	350	450	550	650	750	850	950	1050	1150	1250	1350	1450	1500	Average Velocity	Difference	Percentage
0	0	0	0	0	0	0	0	0	0	0	0	0	0	0	0	0	0			
50	0	5.4	5.6	5.8	5.45	5.43	5.54	5.56	5.58	5.56	5.55	5.43	5.4	5.43	5.41	5.76	0	5.53	0.097	1.72
150	0	5.43	5.64	5.75	5.6	5.6	5.63	5.43	5.45	5.65	5.45	5.63	5.43	5.65	5.4	5.84	0	5.57	0.05	0.92
250	0	5.65	5.65	5.43	5.44	5.53	5.63	5.45	5.63	5.68	5.43	5.44	5.45	5.64	5.6	5.63	0	5.55	0.07	1.27
350	0	5.63	5.5	5.6	5.6	5.67	5.74	5.68	5.83	5.74	5.72	5.7	5.8	5.8	5.9	5.74	0	5.71	-0.09	-1.54
450	0	5.64	5.54	5.74	5.62	5.62	5.63	5.74	5.63	5.83	5.64	5.83	5.74	5.77	5.83	5.83	0	5.71	-0.09	-1.51
550	0	5.7	5.56	5.64	5.5	5.84	5.65	5.65	5.74	5.54	5.63	5.63	5.68	5.55	5.84	5.89	0	5.67	-0.05	-0.81
650	0	5.6	5.6	5.86	5.63	5.73	5.63	5.66	5.84	5.5	5.64	5.38	5.74	5.63	5.45	5.36	0	5.62	0.01	0.12
750	0	5.55	5.64	5.72	5.83	5.43	5.54	5.85	5.84	5.63	5.64	5.6	5.5	5.45	5.65	5.64	0	5.63	-0.01	-0.18
800	0	0	0	0	0	0	0	0	0	0	0	0	0	0	0	0	0			
														Overall Average				5.62		

Table 10 Data for Flow Uniformity at Low Speed

	0	50	150	250	350	450	550	650	750	850	950	1050	1150	1250	1350	1450	1500
0	0	0	0	0	0	0	0	0	0	0	0	0	0	0	0	0	0
50	0	-3.98	-0.42	3.14	-3.09	-3.44	-1.49	-1.13	-0.78	-1.13	-1.31	-3.44	-3.98	-3.44	-3.80	2.42	0
150	0	-3.44	0.29	2.25	-0.42	-0.42	0.11	-3.44	-3.09	0.47	-3.09	0.11	-3.44	0.47	-3.98	3.85	0
250	0	0.47	0.47	-3.44	-3.27	-1.67	0.11	-3.09	0.11	1.00	-3.44	-3.27	-3.09	0.29	-0.42	0.11	0
350	0	0.11	-2.20	-0.42	-0.42	0.82	2.07	1.00	3.67	2.07	1.71	1.36	3.14	3.14	4.91	2.07	0
450	0	0.29	-1.49	2.07	-0.07	-0.07	0.11	2.07	0.11	3.67	0.29	3.67	2.07	2.60	3.67	3.67	0
550	0	1.36	-1.13	0.29	-2.20	3.85	0.47	0.47	2.07	-1.49	0.11	0.11	1.00	-1.31	3.85	4.74	0
650	0	-0.42	-0.42	4.20	0.11	1.89	0.11	0.65	3.85	-2.20	0.29	-4.33	2.07	0.11	-3.09	-4.69	0
750	0	-1.31	0.29	1.71	3.67	-3.44	-1.49	4.02	3.85	0.11	0.29	-0.42	-2.20	-3.09	0.47	0.29	0
800	0	0	0	0	0	0	0	0	0	0	0	0	0	0	0	0	0

Table 11 Data for Medium Speed

	0	50	150	250	350	450	550	650	750	850	950	1050	1150	1250	1350	1450	1500	Average Velocity	Difference	Percentage
0	0	0	0	0	0	0	0	0	0	0	0	0	0	0	0	0	0			
50	0	5.93	5.97	6.02	6.2	5.94	5.83	5.9	5.94	5.94	5.92	5.7	5.84	5.88	5.84	5.84	0	5.91	-0.07	-1.09
150	0	5.95	6.03	6.14	6.15	6.05	5.94	5.94	5.83	5.72	5.87	5.84	5.92	5.6	5.83	5.8	0	5.91	-0.07	-1.18
250	0	5.93	6.02	6.02	6.2	6.01	6.17	6.28	6.22	6.05	5.94	5.98	5.8	5.9	5.94	5.74	0	6.01	0.04	0.60
350	0	5.86	5.8	5.84	5.94	5.83	5.98	6.04	6.1	6.15	5.94	5.9	5.83	5.95	5.72	5.94	0	5.92	-0.06	-0.94
450	0	5.94	5.98	5.9	5.92	6.1	6.12	6.08	6.11	6.15	6.2	5.94	5.84	5.83	5.84	5.94	0	5.99	0.01	0.25
550	0	6.05	6.2	6.14	6.15	6.02	6.3	6.22	6.23	6.08	6.01	5.8	5.95	5.92	5.63	5.74	0	6.03	0.05	0.86
650	0	6.13	6.08	6.03	6.11	6.06	6.18	6.17	6.05	6.15	6.06	6.02	5.98	5.95	6.01	5.81	0	6.05	0.07	1.25
750	0	5.94	6.06	6.04	6.06	5.96	5.92	5.94	6.05	5.93	6.01	5.98	6.1	6.02	5.96	5.92	0	5.99	0.01	0.25
800	0	0	0	0	0	0	0	0	0	0	0	0	0	0	0	0	0			
														Overall Average				5.98		

Table 12 Data for Flow Uniformity at Medium Speed

	0	50	150	250	350	450	550	650	750	850	950	1050	1150	1250	1350	1450	1500
0	0	0	0	0	0	0	0	0	0	0	0	0	0	0	0	0	0
50	0	-0.80	-0.13	0.71	3.72	-0.63	-2.47	-1.30	-0.63	-0.63	-0.97	-4.65	-2.30	-1.64	-2.30	-2.30	0
150	0	-0.46	0.87	2.71	2.88	1.21	-0.63	-0.63	-2.47	-4.31	-1.80	-2.30	-0.97	-6.32	-2.47	-2.97	0
250	0	-0.80	0.71	0.71	3.72	0.54	3.22	5.06	4.05	1.21	-0.63	0.04	-2.97	-1.30	-0.63	-3.98	0
350	0	-1.97	-2.97	-2.30	-0.63	-2.47	0.04	1.04	2.05	2.88	-0.63	-1.30	-2.47	-0.46	-4.31	-0.63	0
450	0	-0.63	0.04	-1.30	-0.97	2.05	2.38	1.71	2.21	2.88	3.72	-0.63	-2.30	-2.47	-2.30	-0.63	0
550	0	1.21	3.72	2.71	2.88	0.71	5.39	4.05	4.22	1.71	0.54	-2.97	-0.46	-0.97	-5.82	-3.98	0
650	0	2.55	1.71	0.87	2.21	1.38	3.38	3.22	1.21	2.88	1.38	0.71	0.04	-0.46	0.54	-2.81	0
750	0	-0.63	1.38	1.04	1.38	-0.30	-0.97	-0.63	1.21	-0.80	0.54	0.04	2.05	0.71	-0.30	-0.97	0
800	0	0	0	0	0	0	0	0	0	0	0	0	0	0	0	0	0

Table 13 Data for Flow Velocity at High Speed

	0	50	150	250	350	450	550	650	750	850	950	1050	1150	1250	1350	1450	1500	Average Speed	Difference	Percentage
0	0	0	0	0	0	0	0	0	0	0	0	0	0	0	0	0	0			
50	0	6.2	5.97	6.02	6.25	6.32	6.39	6.41	6.27	6.44	5.97	6.05	5.92	6.15	6.24	6.16	0	6.18	-0.12	-1.92
150	0	6.25	6.35	6.43	6.44	6.64	6.5	6.45	6.54	6.55	6.48	6.57	6.34	6.42	6.34	6.39	0	6.45	0.14	2.24
250	0	6.14	6.35	6.3	6.4	6.01	6.17	6.54	6.48	6.38	6.43	6.65	6.52	6.41	6.4	6.34	0	6.37	0.06	1.00
350	0	6.34	6.43	6.56	6.38	6.52	6.64	6.6	6.55	6.52	6.62	6.64	6.49	6.58	6.64	6.25	0	6.52	0.21	3.37
450	0	6.38	6.24	6.38	6.54	6.48	6.45	6.64	6.56	6.38	6.63	6.5	6.55	6.31	6.48	6.16	0	6.45	0.14	2.23
550	0	6.28	6.54	6.31	6.27	6.34	6.26	6.15	6.05	6.08	6.43	6.26	6.41	6.26	6.37	6.02	0	6.27	-0.04	-0.57
650	0	6.13	6.08	6.25	6.11	6.06	6.18	6.4	6.27	6.15	6.06	6.02	5.98	5.95	6.01	6.04	0	6.11	-0.19	-3.05
750	0	6.05	6.2	6.34	6.32	6.24	6.3	6.01	6.05	5.93	6.01	5.98	6.1	6.02	5.96	5.95	0	6.10	-0.21	-3.29
800	0	0	0	0	0	0	0	0	0	0	0	0	0	0	0	0	0			
													Overall Average					6.30		

Table 14 Data for Flow Uniformity at High Speed

	0	50	150	250	350	450	550	650	750	850	950	1050	1150	1250	1350	1450	1500
0	0	0	0	0	0	0	0	0	0	0	0	0	0	0	0	0	0
50	0	-1.66	-5.31	-4.52	-0.87	0.24	1.35	1.67	-0.55	2.14	-5.31	-4.04	-6.11	-2.46	-1.03	-2.30	0
150	0	-0.87	0.72	1.98	2.14	5.31	3.09	2.30	3.73	3.89	2.78	4.20	0.56	1.83	0.56	1.35	0
250	0	-2.62	0.72	-0.08	1.51	-4.68	-2.14	3.73	2.78	1.19	1.98	5.47	3.41	1.67	1.51	0.56	0
350	0	0.56	1.98	4.05	1.19	3.41	5.31	4.68	3.89	3.41	5.00	5.31	2.94	4.36	5.31	-0.87	0
450	0	1.19	-1.03	1.19	3.73	2.78	2.30	5.31	4.05	1.19	5.16	3.09	3.89	0.08	2.78	-2.30	0
550	0	-0.40	3.73	0.08	-0.55	0.56	-0.71	-2.46	-4.04	-3.57	1.98	-0.71	1.67	-0.71	1.03	-4.52	0
650	0	-2.77	-3.57	-0.87	-3.09	-3.88	-1.98	1.51	-0.55	-2.46	-3.88	-4.52	-5.15	-5.63	-4.68	-4.20	0
750	0	-4.04	-1.66	0.56	0.24	-1.03	-0.08	-4.68	-4.04	-5.95	-4.68	-5.15	-3.25	-4.52	-5.47	-5.63	0
800	0	0	0	0	0	0	0	0	0	0	0	0	0	0	0	0	0

APPENDIX C:

FABRICATION AND EXPERIMENTAL SETUP

Figure 42 Fabrication of Frame to hold Multiple Fan

Figure 43 Overall Wind Tunnel

Figure 44 Initial Setup to observe Roll

Figure 45 Initial Setup to observe Pitch

Design, Fabrication and Performance Evaluation of Low Speed Open Jet Wind Tunnel

ORIGINALITY REPORT

12%
SIMILARITY INDEX

PRIMARY SOURCES

1	www.researchgate.net Internet	140 words — 2%
2	en.wikipedia.org Internet	135 words — 2%
3	David Greenblatt. "Development and Testing of an Unsteady Low-Speed Wind Tunnel", 31st AIAA Aerodynamic Measurement Technology and Ground Testing Conference, 2015 Crossref	85 words — 1%
4	spectrum.library.concordia.ca Internet	69 words — 1%
5	link.springer.com Internet	63 words — 1%
6	Stathopoulos, T.. "Design and fabrication of a wind tunnel for building aerodynamics", Journal of Wind Engineering & Industrial Aerodynamics, 198404 Crossref	57 words — 1%
7	www.intechopen.com Internet	48 words — 1%

8	Huang, Jinglin. "Investigations of Different Methods to Promote Drug Mixing in the Eye.", California Institute of Technology, 2023 ProQuest	20 words — < 1%
9	pdfcoffee.com Internet	20 words — < 1%
10	users.df.uba.ar Internet	20 words — < 1%
11	Vlahakis, James K. "Chemical mechanical planarization: Synchronous, in situ measurements of the coefficient of friction, wafer orientation and material removal rate", Proquest, 20111004 ProQuest	19 words — < 1%
12	digitalcommons.usf.edu Internet	18 words — < 1%
13	WILLIAM SELLERS, III, SCOTT KJELGAARD. "The Basic Aerodynamics Research Tunnel - A facility dedicated to code validation", 15th Aerodynamic Testing Conference, 1988 Crossref	17 words — < 1%
14	www.mdpi.com Internet	17 words — < 1%
15	iasj.net Internet	16 words — < 1%
16	Itimad D J Azzawi. "Design and characterizing of blower wind tunnel using experimental and numerical simulation", Proceedings of the Institution of Mechanical Engineers, Part G: Journal of Aerospace Engineering, 2023	15 words — < 1%

Crossref

17 Juan Carlos Serrano Rico, Filipe R. Amaral, Christian Bresci, Matheus M. Beraldo, Marcello F. Medeiros. "Low Acoustic Noise and Turbulence (LANT) wind-tunnel at USP-EESC", 2018 Applied Aerodynamics Conference, 2018 — 15 words — < 1%
Crossref

18 arxiv.org — 14 words — < 1%
Internet

19 K. P. Neriya Hegade, R. Natalia, B. Wehba, A. Mittal, R. B. Bhat, M. Packirisamy. "Design and study of mini wind tunnel for microsystems fluid interaction under low Reynolds number flows", SN Applied Sciences, 2020 — 13 words — < 1%
Crossref

20 Sai Sravan Yarlagadda, Siddharth Sriram Sikha, Gaurav Kumar Pandey, Pedi Reddi Varshith, Edison Gundabattini. "Utilization of Wind Tunnels for Subsonic and Transonic Flow for Aeronautical and Non-aeronautical Applications: A Review", Journal of The Institution of Engineers (India): Series C, 2021 — 13 words — < 1%
Crossref

21 A. Gan Chowdhury, I. Zisis, P. Irwin, G. Bitsuamlak, J.-P. Pinelli, B. Hajra, M. Moravej. "Large-Scale Experimentation Using the 12-Fan Wall of Wind to Assess and Mitigate Hurricane Wind and Rain Impacts on Buildings and Infrastructure Systems", Journal of Structural Engineering, 2017 — 12 words — < 1%
Crossref

22 www.frontiersin.org — 12 words — < 1%
Internet

23	sportdocbox.com Internet	11 words — < 1%
24	Salem S. Abdel Aziz, Essam B. Moustafa, Abdel-Halim Saber Salem Said. "Experimental Investigation of the Flow, Noise, and Vibration Effect on the Construction and Design of Low-Speed Wind Tunnel Structure", Machines, 2023 Crossref	10 words — < 1%
25	mafiadoc.com Internet	10 words — < 1%
26	monolith.asee.org Internet	10 words — < 1%
27	www.eng.fiu.edu Internet	10 words — < 1%
28	Feroz, Muhammad Zubair. "Mathematical Modelling of Unsteady Wind Tunnels.", Illinois Institute of Technology, 2018 ProQuest	9 words — < 1%
29	Karava, Panagiota. "Airflow prediction in buildings for natural ventilation design: Wind tunnel measurements and simulation", Proquest, 20111003 ProQuest	9 words — < 1%
30	core.ac.uk Internet	9 words — < 1%
31	ijera.com Internet	9 words — < 1%
32	mech.pcampus.edu.np Internet	9 words — < 1%

33 Mirza, Fahad. "Investigation of the impact response of lead-free electronic assemblies and comparison of drop with cyclic 4-point bend test", Proquest, 20111108 — 8 words — < 1%
ProQuest

34 Ziad Azzi, Amal Elawady, Peter Irwin, Arindam Gan Chowdhury, Caesar Abi Shdid. "Aeroelastic modeling to study the wind-induced response of a self-supported lattice tower", Engineering Structures, 2021 — 8 words — < 1%
Crossref

35 ntrs.nasa.gov — 8 words — < 1%
Internet

36 David Greenblatt. "Unsteady Low-Speed Wind Tunnels", AIAA Journal, 2016 — 7 words — < 1%
Crossref

37 Longhua Hu. "A review of physics and correlations of pool fire behaviour in wind and future challenges", Fire Safety Journal, 2017 — 7 words — < 1%
Crossref

38 "Chapter 300925 WEC: Wave Energy Converter", Springer Science and Business Media LLC, 2022 — 6 words — < 1%
Crossref

39 Bert Celis, Harm H. Ubbens. "Design and Construction of an Open-circuit Wind Tunnel with Specific Measurement Equipment for Cycling", Procedia Engineering, 2016 — 6 words — < 1%
Crossref

40 Johnny Chun-Chau Sung, Pak-Long Wu, Ellis Yung-Mau So, Kam-Chau Wu et al. "Assessment of novel — 6 words — < 1%

antiviral filter using pseudo-type SARS-CoV-2 virus in fast air velocity vertical-type wind tunnel", Scientific Reports, 2023
Crossref

41 Jorge Saavedra, Guillermo Paniagua, Francisco Lozano, Jordan Fisher, Austin Webb, Terrence Meyer. "Flow conditioning system for tri-sonic high pressure aerothermal testing", Flow Measurement and Instrumentation, 2021 — 6 words — < 1%
Crossref

42 RICHARD MILLS, JOHN SHERIDAN, KERRY HOURIGAN. "Response of base suction and vortex shedding from rectangular prisms to transverse forcing", Journal of Fluid Mechanics, 2002 — 6 words — < 1%
Crossref

43 Ziad Azzi, Filmon Habte, Krishna Sai Vutukuru, Arindam Gan Chowdhury, Mohammadtaghi Moravej. "Effects of roof geometric details on aerodynamic performance of standing seam metal roofs", Engineering Structures, 2020 — 6 words — < 1%
Crossref

EXCLUDE QUOTES	ON	EXCLUDE SOURCES	< 6 WORDS
EXCLUDE BIBLIOGRAPHY	ON	EXCLUDE MATCHES	OFF